

Investigation of anomalous thermodynamic and transport properties of $\text{Sr}_{1-x}\text{Ca}_x\text{RuO}_3$ ($x \geq 0.8$)

A. Zarzycki,¹ M. Rams,² E. A. Görlich,² and K. Tomala²

¹*H. Niewodniczański Institute of Nuclear Physics, Polish Academy of Science, Radzikowskiego 152, 31-342 Kraków, Poland*

²*M. Smoluchowski Institute of Physics, Jagiellonian University, Łojasiewicza 11, 30-348 Kraków, Poland*

(Dated: May 8, 2018)

Thermodynamic and transport properties of $\text{Sr}_{1-x}\text{Ca}_x\text{RuO}_3$ with a calcium concentration $x \geq 0.8$ were investigated at low temperatures and in external magnetic field. The investigations revealed a Landau Fermi liquid (LFL) behaviour characterized by specific heat $C/T = \text{const}$ and resistivity $\rho \sim T^2$ and an anomalous non-Fermi liquid (NFL) behaviour with $\rho \sim T^{5/3}$ and a quasi-logarithmic increase of C/T with decreasing temperature. The T - x and T - B phase diagrams which separate both regions were prepared for the investigated materials. Then, the experimental behaviour of C/T and $\rho(T)$ were compared with predictions of the self-consistent renormalization (SCR) theory of spin fluctuations. Within this approach, $C/T(T)$ was well described up to 20 K. The SCR parameters y_0 , y_1 and T_0 inferred from specific heat analysis allowed to describe properly $\rho(T)$ up to approximately 5 K. In addition, the resistivity data were analysed within the 'hidden Fermi liquid' theory of Anderson, obtaining very good description of the experimental behaviour up to about 25 K. An anomalous increase of the C/T ratio already in the LFL region below 2 K in very weak magnetic fields (0.2–0.3 T) was identified as caused by the Schottky anomaly induced by ferromagnetic clusters embodied into the essentially paramagnetic materials.

PACS numbers: 75.30.Kz, 75.40.-s, 72.15.Gd, 71.10.Hf

I. INTRODUCTION

Almost to the end of the 20-th century the physical properties of correlated metals at low temperatures were successfully described within the phenomenological Landau's theory of the Fermi liquid (LFL). The Fermi liquid theory assumes existence of the one-to-one correspondence between single particle excitations of a free electron gas and those of interacting electrons. These excitations which carry the same charge, momentum and spin as free electrons are called quasiparticles. The correspondence between the excitations spectra leads to similar behavior of thermodynamic parameters such as the electronic specific heat $C/T = \gamma = \text{const}$ and the magnetic susceptibility $\chi = \text{const}$. The temperature dependence of the resistivity is given by the formula $\rho = \rho_0 + AT^2$, where ρ_0 is a residual resistivity.¹ Since γ and χ are proportional to the density of states at the Fermi energy, both of them are proportional to an effective mass m^* of the quasiparticles. The constant A in the resistivity formula is proportional to $(m^*)^2$. Therefore, a linear correlation between A and γ^2 , found for a considerable group of different materials, proves legitimacy of this approach.² This correlation has been recently improved for heavy fermion cerium and ytterbium compounds, taking into account a degeneracy of the electronic 4f shell.³

Nevertheless, during the last years numerous systems which show distinct deviations from the Landau's Fermi liquid phenomenology have been discovered. These systems are known as non-Fermi liquid (NFL) materials or as the materials that show the non-Fermi liquid behaviour. Their anomalous properties are often characterized by a continuous increase of the electronic specific heat coefficient γ with decreasing temperature, as

well as by distinct deviation from the T^2 temperature dependence of the electrical resistivity.⁴ It appears that these anomalous properties are very often observed in the systems which are close to quantum phase transitions (QPT), i.e. the phase transitions that take place at zero temperature. In contradistinction to classical phase transitions where thermal fluctuations are responsible for the phase transformation, the quantum phase transitions are driven by quantum fluctuations of an order parameter. Pressure, magnetic field or concentration of components in heterogeneous materials are usually used to tune the system to the region of QPT. The anomalous properties usually cover a large part of the phase diagram making possible their experimental detection and characterization at higher temperatures.⁵ As in the case of the classical phase transitions one can distinguish a first order (discontinuous) and a second order (continuous) transitions.

First of all, the investigations of the NFL properties concentrated mostly on the heavy fermion materials in the vicinity of the QPT between an antiferromagnetic (AF) and a paramagnetic (PM) states. As the best studied examples one should mention $\text{CaCu}_{6-x}\text{Au}_x$ system with $x \simeq 0.1$ where the pressure, the concentration of components or the external magnetic field were applied as tuning parameters⁶ and YbRh_2Si_2 which shows the AF order with the Néel temperature of $T_N \simeq 70$ mK but can be tuned to the quantum critical point by a relatively weak external magnetic field.⁷ Both systems at low temperatures show the anomalous behaviour of the specific heat $C/T \sim -\log T$ and the resistivity $\rho \sim T$ over more than a decade of temperature.

The important group of materials in which the magnetically ordered state can be tuned to the paramagnetic

state by variations of the pressure or the composition is formed by weak itinerant ferromagnets. Among the numerous investigated materials one can mention the probably most representative clean systems: MnSi ,⁸ ZrZn_2 ,⁹ and NiAl_3 ¹⁰ as well as the systems with a quenched disorder: $\text{Ni}_{1-x}\text{Pd}_x$,¹¹ $\text{Zr}_{1-x}\text{Nb}_x\text{Zn}_2$,¹² and $\text{Ni}_3\text{Al}_{1-x}\text{Ga}_x$.¹³ The $\text{Sr}_{1-x}\text{Ca}_x\text{RuO}_3$ system, which is the subject of studies presented in this paper, can be included in the last group. Recently, the results of investigations of the metallic systems being on the border of itinerant magnetism and metallic paramagnetism were gathered and discussed in the extensive review paper.¹⁴

The magnetic properties of the $\text{Sr}_{1-x}\text{Ca}_x\text{RuO}_3$ compounds were already seriously investigated and a significant number of publications have appeared up to now.^{15–20} The system shows a complete solid solubility for the entire range of concentrations. The increase of the calcium concentration is connected with increase of the orthorhombic GdFeO_3 type distortion of the cubic perovskite lattice leading to increased buckling of the Ru-O-Ru bond which is probably responsible for the magnetic behaviour.²¹ The pure strontium and calcium compounds show distinctly different magnetic behaviour. SrRuO_3 is a metallic ferromagnet with the Curie temperature $T_C \simeq 160$ K, a paramagnetic Curie temperature $\Theta_p \simeq 160$ K and a spontaneous magnetic moment $\mu_s \simeq 0.84\mu_B$ per Ru atom, the last one being rather far from the expected magnetic moment of the Ru^{4+} ion with a $4d^4$ configuration in a low spin state with $S = 1$.¹⁹ Substitution of Sr^{2+} ions by smaller Ca^{2+} leads to the gradual decrease of the Curie temperatures and simultaneously to decrease of the ruthenium magnetic moments. For a long time there was common consent that the ferromagnetic order disappears at some critical concentration near $x_{cr} \simeq 0.7$ that was obtained by an extrapolation of the concentration dependence of $T_C(x)$ for the compounds on the strontium rich side. For $\text{Sr}_{0.4}\text{Ca}_{0.6}\text{RuO}_3$, classified still as a homogenous ferromagnet (for an explanation see below), $T_C \simeq 25$ K and $\mu_s \simeq 0.16\mu_B$ per Ru atom. The temperature dependence of the magnetic susceptibilities at high temperatures (approximately above 60–80 K), for all $\text{Sr}_{1-x}\text{Ca}_x\text{RuO}_3$ compounds can be well described by the Curie-Weiss formula. Nevertheless, drastic decrease of the paramagnetic Curie temperatures Θ_p is observed which for materials with $x \gtrsim 0.6$ become negative. However, the paramagnetic magnetic moments are relatively constant and show only a minor increase from $\mu_{eff} \simeq 2.7\mu_B$ in SrRuO_3 to above $\mu_{eff} \simeq 3.0\mu_B$ for calcium rich materials. In spite of the very large negative paramagnetic Curie temperature $\Theta_p \simeq -150$ K which could suggest the antiferromagnetic order and $\mu_{eff} \simeq 3.4\mu_B$ at high temperatures, CaRuO_3 does not order magnetically.^{18,19,22–24} It was classified as a strongly exchange enhanced paramagnet (Stoner enhancement factor $\alpha \simeq 0.97$) on the border of ferromagnetism.²² The magnetic investigations performed in our Laboratory and shown in the Supplemental materials allow to conclude that the $\text{Sr}_{1-x}\text{Ca}_x\text{RuO}_3$

compounds with the calcium concentrations $x \geq 0.8$ are essentially paramagnetic.

This short review shows that the magnetic properties of $\text{Sr}_{1-x}\text{Ca}_x\text{RuO}_3$ cannot be described as ordering of the magnetic moments localized at ruthenium atoms. They show the distinct features of the itinerant magnetism and the zero temperature transition around $x_{cr} \simeq 0.7$ occurs between the itinerant ferromagnet and the paramagnetic metal.

Important information about the magnetic behaviour of $\text{Sr}_{1-x}\text{Ca}_x\text{RuO}_3$ and especially about the concentration tuned quantum phase transition were inferred from the precise magnetisation measurements using a magneto-optical Kerr rotation method for a thin epitaxial film with practically continuous variation of the calcium concentration.²⁵ It has appeared that the strong crystallographic distortion caused by different radii of the Sr and Ca atoms leads to significant extension of the ferromagnetic phase over a wide range of compositions x which can be understood as caused by formation of an inhomogeneous ferromagnetic state built up of frozen magnetic clusters embodied into the paramagnetic metal. There is no any abrupt change of the Curie temperature on the T - x phase diagram, which means that the composition tuned quantum transition between the ferromagnetic and paramagnetic phases in $\text{Sr}_{1-x}\text{Ca}_x\text{RuO}_3$ is smeared and practically destroyed by the strong crystallographic disorder. It means that instead of a single critical concentration $x_{cr} \simeq 0.7$ there exists rather a critical range of concentrations within which the transition takes place. In the following parts of the text we sometimes use a notion ‘critical concentration of the phase transition’ (usually written in the quotation mark), nevertheless, one should always understand it as a critical range of concentrations.

In order to finish this short review of the magnetic properties of $\text{Sr}_{1-x}\text{Ca}_x\text{RuO}_3$ perovskites one should also consider the results of the investigations using different microscopic methods like muon spin rotation (μSR),^{26,27} ^{16}O and ^{99}Ru nuclear magnetic resonances (NMR)^{18,22} and neutron scattering (NS).²⁸

A very important piece of information provided by the μSR experiments concerns the existence of a phase separation in $\text{Sr}_{1-x}\text{Ca}_x\text{RuO}_3$ for compositions with the calcium concentration $x \geq 0.65$, just around the recently discussed ‘critical concentration’ at $x_{cr} \simeq 0.7$. The compounds in this range of concentrations are magnetically inhomogeneous and contain both ferromagnetic and paramagnetic fractions. This result is in agreement with the suggestion of the inhomogeneous magnetic state inferred from the thin film magnetisation measurements.²⁵ Both NMR and NS are sensitive to the dynamics of the magnetic moments. The NMR investigations allowed to discover very strong ferromagnetic spin fluctuations for $\text{Sr}_{1-x}\text{Ca}_x\text{RuO}_3$ compounds in the whole range of calcium concentrations including pure CaRuO_3 , in spite of the large negative paramagnetic Curie temperature in this compound.¹⁸ The spin fluctuations in CaRuO_3 were also

discovered by the inelastic neutron scattering.²⁸ In addition, detailed analysis of the neutron scattering profile suggests ‘the formation of small ferromagnetic domains, behaving as dynamic paramagnetic clusters of Ru^{4+} spins’.

An important difference between strontium and calcium compounds concerns not only the magnetic behaviour but also their thermodynamic and transport properties. SrRuO_3 demonstrates the LFL behaviour with $\rho \sim T^2$ at low temperatures^{29,30} and $C/T = \text{const}$ with the enhanced electronic specific heat coefficient $\gamma \simeq 30 \text{ mJ/molK}^2$.^{16,30–33} The LFL properties are preserved after substitution of Sr^{2+} ions by Ca^{2+} at least to the calcium concentration $x \simeq 0.6$, that means for samples which are ferromagnetically ordered.³⁰ However, the paramagnetic samples with the calcium concentration above approximately $x = 0.8$ demonstrate the NFL properties characterized by a temperature dependence of the resistivity different from T^2 and often anomalous behaviour of C/T at low temperatures.^{30,32} The most frequently investigated pure CaRuO_3 shows NFL features both in the resistivity and the specific heat. The results of the resistivity measurements performed on single crystals, thin films and polycrystalline samples above 2 K point to the temperature dependence $\rho \sim T^{3/2}$.^{29,30,34} Only recently, the LFL state was found in CaRuO_3 below 1.5 K with recovery of the anomalous behaviour at higher temperatures.³⁵ The results of the specific heat measurements of CaRuO_3 demonstrate at low temperatures a wide variety of behaviour. Some investigations show only the LFL properties and the specific heat is well described by the linear electronic contribution and a lattice contribution given by the Debye model.^{16,36,37} The other investigations show the anomalous NFL upturn of C/T at low temperatures which was analysed within the spin-fluctuation theory of Moriya (see below),³² the upturn with some mysterious and magnetic field dependent structure around 2 K,³³ and the upturn with the power law temperature dependence down to 100 mK.³⁸ Recently, the continuous increase of C/T with decreasing temperature was reported down to 1.8 K, nevertheless, without any theoretical analysis of C/T for materials with $x \geq 0.7$.²⁰

Simultaneously with the experimental investigations theoretical methods which could allow to understand and describe the deviations from the Landau Fermi liquid behaviour were developed. Since these anomalous behaviours often take place close to the zero temperature phase transitions which are caused by strong quantum fluctuations of the order parameter it suggests that their theoretical description should be connected with the theory of the quantum phase transitions. The first theoretical analysis of the zero temperature phase transition from the itinerant ferromagnet to the paramagnetic metal was performed within the ϕ^4 quantum field theory with the Ginzburg-Landau-Wilson functional which was analysed by the renormalization group (RG) method.⁴⁰ It was found that the quantum phase transition for a sys-

tem with a spatial dimension d can be analysed as classical transition for the system with the effective dimension $d_{\text{eff}} = d + z$, where z is a dynamic critical exponent. In the next step, the theoretical investigations within this framework were extended to higher temperatures and allowed to make predictions about the temperature behaviour of different physical parameters in the critical region for the materials which show FM and AFM orders and of different spatial dimensionality.⁴¹ For example, for the transition between the 3-dimensional itinerant ferromagnet and paramagnetic metal the heat capacity should scale as $C/T \sim -\log T$ and the temperature dependence of the resistivity should behave as $\rho(T) \sim T^{5/3}$. Independently, another theoretical approach used to describe the properties of the itinerant magnets close to the border of the magnetic instability was developed.⁴² This approach stresses importance of the spin fluctuations both in nearly magnetic and magnetically ordered FM^{43,46} or AFM⁴⁷ states. The theory, called the self-consistent renormalization (SCR) theory of spin fluctuations, predicts the phase diagrams and the temperature variation of many physical parameters including the magnetic susceptibility, specific heat and electrical resistivity. The same kind of the spin fluctuation theory was independently developed by another authors.⁴⁴ The results of the theoretical investigations in the critical region of the magnetic instabilities were gathered in the already quoted extended review article.⁴

Here we report the results of the zero field and magnetic field tuned specific heat and electrical resistivity investigations of $\text{Sr}_{1-x}\text{Ca}_x\text{RuO}_3$ compounds which are in the paramagnetic phase above the zero temperature phase transformation. Since in the region around the discussed ‘critical concentration’ ($x \simeq 0.7$) the compounds are magnetically inhomogeneous we confined the studies to the materials with the compositions $x = 0.8, 0.9$, and 1.0 . They are still quite close to the region of concentrations where the ferromagnetic to paramagnetic transformation takes place at zero temperature but simultaneously they are homogeneously paramagnetic. The conclusion about their paramagnetic behaviour can be drawn from the results of the bulk magnetic measurements presented in Supplemental materials where the results of investigations performed for the compounds within the extended range of compositions from $x = 0.60$ up to $x = 1.0$ are reported. They prove that in general the materials with the calcium concentration $x \geq 0.8$ are paramagnetic, at least down to 2 K.⁴⁹ These do not exclude a possible existence of a small amount of ferromagnetic clusters which can strongly influence the magnetic properties at low temperatures. Since no any irregularities in the temperature dependences of the specific heat down to 0.4 K and the electrical resistivity down to approximately 0.7 K were detected it seems that they do not show any magnetic order to much lower temperatures. The essentially paramagnetic behaviour of the $x = 0.8$ sample is also strongly supported by the results of a ^{99}Ru Mössbauer effect investigations which are shown in the

Supplemental materials.

The experimental results were analysed in a few ways. First of all, the Fermi liquid region was identified using C/T and $\rho(T)$ behaviour and the phase diagrams on the T - x and T - B planes were prepared, which demonstrate the regions of FL and NFL properties. Then, the results of C/T and $\rho(T)$ were compared with the predictions of the Moriya's SCR theory of spin fluctuations^{42,46} and with the 'hidden Fermi liquid' theory of Anderson.⁴⁸ At the end, we provide a summary of the experimental results and present the conclusions inferred from their analysis.

II. EXPERIMENTAL DETAILS

The polycrystalline $\text{Sr}_{1-x}\text{Ca}_x\text{RuO}_3$ compounds with a few calcium concentrations between $x = 0.60$ and 1.0 were prepared by the solid state reaction from weighted in a proper molar ratios RuO_2 , SrCO_3 and CaCO_3 . First of all, mixed and pressed powders were calcined for several hours at 800°C . Then, after grinding, they were pressed into pellets under high pressure and sintered at high temperatures for approximately 15 hours. The compounds with the calcium concentrations between $x = 0.60$ and 0.80 were sintered at 1300°C and the grinding procedure was repeated several times (at least 3 times). The materials with $x = 0.9$ and 1.0 were sintered in sequence at 1000°C , 1100°C and 3 times at 1200°C . All heat treatments were performed in the atmosphere of flowing $\text{Ar} + 1\%\text{O}_2$. After sintering the samples were cooled down with the furnace.

The crystal structures of the prepared materials were verified by the X-ray diffraction using the Cu K_α radiation and D501 Siemens powder diffractometer. The diffraction patterns were analysed using the FULLPROF program within the $Pnma$ space group, which describes the perovskite structure with orthorhombic distortion of the GdFeO_3 type. It was found that all synthesized materials were single phase.

Due to the observation of the smeared zero temperature ferromagnetic to paramagnetic phase transition and the inhomogeneous magnetic state in the critical region discovered by the μSR measurements^{25,26} the investigations of the bulk magnetic properties were used to select materials which being close to the region of the phase transformation were still paramagnetic. The magnetization measurements for the compounds within the concentration range from $x = 0.6$ up to 1.0 were performed using MPMS XL5 SQUID magnetometer from Quantum Design including low field susceptibility ($B \simeq 5$ mT), ac susceptibility, hysteresis loop at 2 K and study of the magnetic equation of state (Arrott plot). These measurements allowed to conclude that the compounds with the calcium concentrations $x \geq 0.8$ are essentially paramagnetic, at least down to 2 K. The results of these investigations are presented in the Supplemental materials. The Supplemental materials contain also the results of ^{99}Ru

Mössbauer effect investigations of the compounds with compositions $x = 0.6$ and 0.8 . They confirm the paramagnetism of the $x = 0.8$ compounds (at least down to 4.2 K) and the homogenous ferromagnetism of the $x = 0.6$ material where homogenous means that all ruthenium magnetic moments take part in the ferromagnetic ordering. Taking into account the results of all these investigations, $\text{Sr}_{1-x}\text{Ca}_x\text{RuO}_3$ compounds with the compositions $x = 0.8, 0.9$, and 1.0 were selected for further studies of the thermodynamic and transport properties.

The specific heat and the electrical resistivity measurements were performed using the PPMS equipment from Quantum Design with the ^3He option and 9 T superconducting magnet. This equipment in our case allowed to carry out the specific heat measurements with the required accuracy in the range of temperatures down to 0.4 K in the external magnetic fields up to 3 T. The Apiezon N grease was used to fix the samples in the microcalorimeter. Its heat capacity was measured for each sample at each magnetic field, and then subtracted. The smooth calibration of microcalorimeter thermometers occurred to be very important to obtain reproducible and smooth specific heat dependences.

The dc current option of the the resistivity measurements allowed to perform the measurements down to 0.6–0.7 K in the full range of the accessible magnetic fields.

III. EXPERIMENTAL RESULTS AND ANALYSIS

In this section, the results of the investigation of the specific heat and the electrical resistivity are presented. In the first part, the zero field measurements are shown and used to prepare a phase diagram which separates on the T - x plane the regions of FM, LFL and NFL properties. The LFL region was defined by the Landau Fermi liquid temperature T_{LFL} derived from the upper limit of $C/T = \text{const}$ behaviour in the specific heat and from the upper limit of the $\rho \sim T^2$ temperature dependence of the resistivity. Then, the phase diagrams on the T - B plane for all the investigated compounds are prepared from the results of the specific heat and resistivity measurements in the external magnetic field. Since the dc current method of the resistivity measurements used in our PPMS system has not enough accuracy to identify without any doubt the upper limit of $\rho \sim T^2$ dependence below approximately 2 K (an exception is the $\rho(T)$ dependence in CaRuO_3 at zero field) in this range of temperatures only the results of the specific heat measurements were used to identify the LFL properties. On the contrary, in the external magnetic fields above 3 T when the LFL region growth to much higher temperatures the T_{LFL} temperature can be determined from the results of the resistivity measurements. In the NFL region the specific heat follows the quasi-logarithmic behaviour and the electrical resistivity was analysed using the $\rho \sim T^{5/3}$ relation.

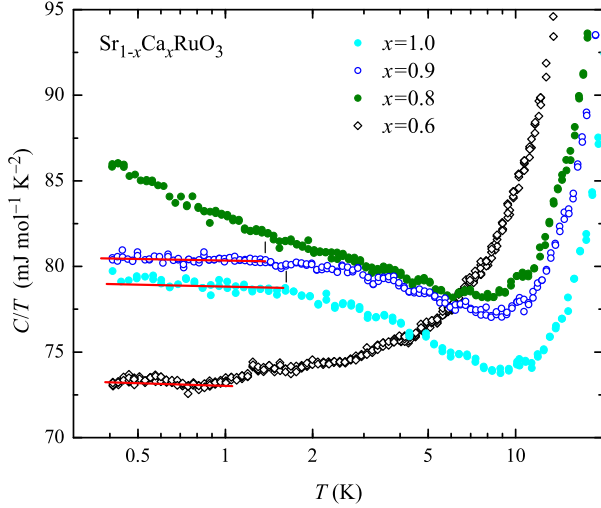


FIG. 1: (Color online) Temperature dependence of specific heat C measured in zero magnetic field for several compositions of $\text{Sr}_{1-x}\text{Ca}_x\text{RuO}_3$. The constant C/T , as marked by red lines, indicate LFL behaviour.

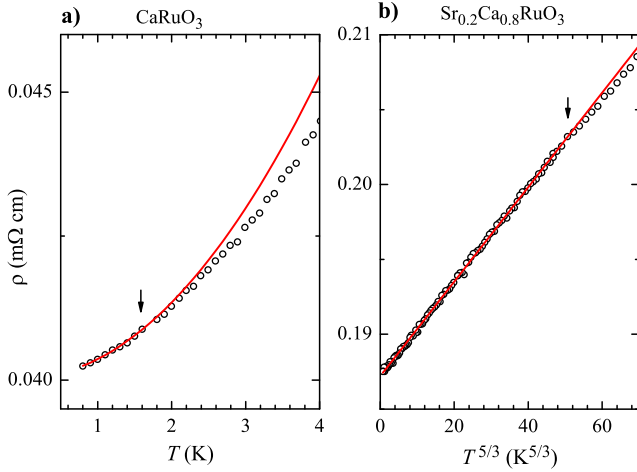


FIG. 2: (Color online) Temperature dependencies of electrical resistivity for CaRuO_3 (a) and for $\text{Sr}_{0.2}\text{Ca}_{0.8}\text{RuO}_3$ (b). The solid lines were fitted using T^2 and $T^{5/3}$ laws, respectively.

A. Zero field specific heat and resistivity

The temperature behaviour of the specific heat presented as C/T versus $\log T$ for the compounds with the calcium concentrations $x = 0.6, 0.8, 0.9$, and 1.0 is shown in Fig. 1. At first, one can directly confirm that the ground states of $\text{Sr}_{0.1}\text{Ca}_{0.9}\text{RuO}_3$ and CaRuO_3 are the Landau Fermi liquids. In both materials the $C/T = \text{const}$ behaviour extends above 1 K. Identification of the LFL ground state in CaRuO_3 below $T_{LFL} = 1.60(15)$ K is in good agreement with the recently published results of the resistivity measurements $T_{LFL} = 1.5$ K³⁵ and with the results of our transport investigations which

give $T_{LFL} = 1.6(2)$ K (see below). The temperature dependence of specific heat for $\text{Sr}_{0.2}\text{Ca}_{0.8}\text{RuO}_3$ is distinctly different and C/T increases to the lowest accessible temperature. The reason of this anomalous increase will be discussed in one of the following sections. However, one cannot exclude a recovery of the LFL state at lower temperatures (see the results of the specific heat measurements in external magnetic fields shown in the next section), nevertheless, it could appear only below approximately 0.5 K. For comparison, we present also the results of the specific heat measurements for the $x = 0.6$ sample which is the homogenous ferromagnet and shows the LFL properties.^{26,30}

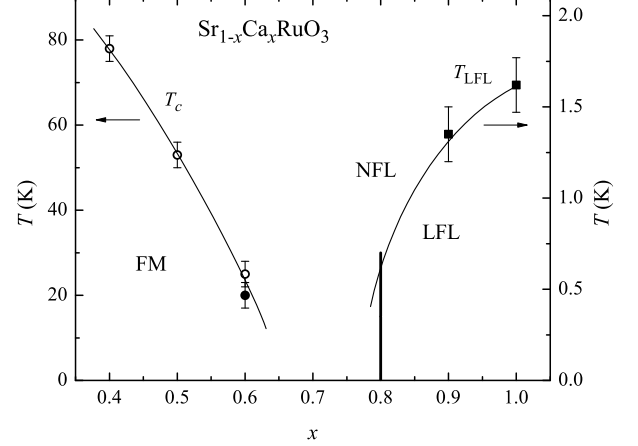


FIG. 3: T - x phase diagram for $\text{Sr}_{1-x}\text{Ca}_x\text{RuO}_3$ with regions of ferromagnetic (FM), Landau Fermi liquid (LFL) and non-Fermi liquid (NFL) behaviour.

The conclusions inferred from the temperature variations of the specific heat are corroborated by the results of the electrical resistivity measurements. In Fig. 2 the zero field $\rho(T)$ dependence for CaRuO_3 and $\text{Sr}_{0.2}\text{Ca}_{0.8}\text{RuO}_3$ are shown. For CaRuO_3 is well described by the $\rho(T) = \rho_0 + a_2 T^2$ formula. This formula fitted to experimental points below 1.6 K is in Fig. 2a extended to higher temperatures to show deviation from the T^2 law above 1.6 K. The temperature dependence of the resistivity for $\text{Sr}_{0.2}\text{Ca}_{0.8}\text{RuO}_3$, shown in Fig. 2b, can be well analysed using the NFL formula $\rho(T) = \rho_0 + a_{5/3} T^{5/3}$ to the lowest accessible in our experiment temperature of 0.7 K.

The experimental results allow to prepare the phase diagram on the T - x plane which indicates FM (for simplicity only the values of T_C for the compounds with the calcium concentrations $x = 0.4, 0.5$ and 0.6 are shown), LFL and NFL phases (Fig. 3).

B. Specific heat and resistivity in external magnetic field

The specific heat behaviour in different external magnetic fields, presented as C/T on the half-logarithmic

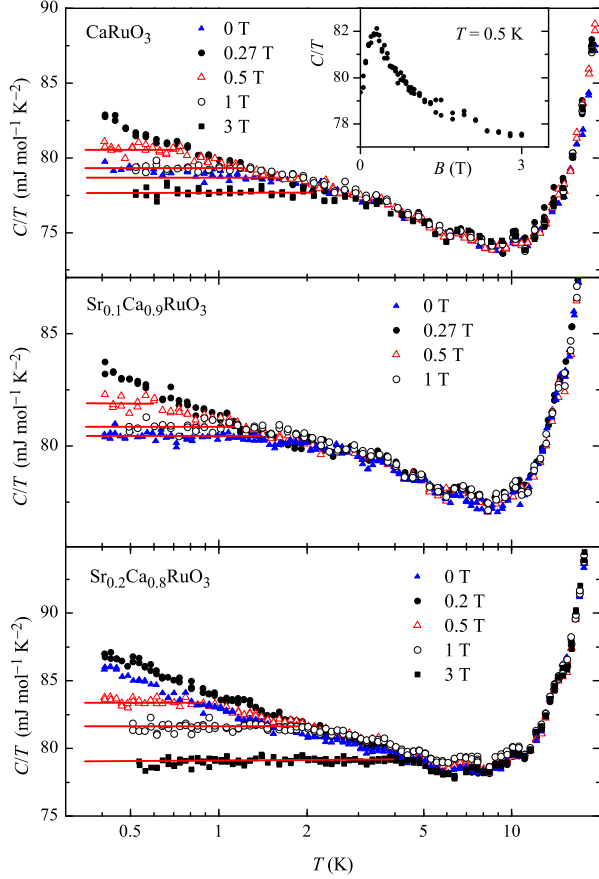


FIG. 4: (Color online) Temperature dependence of specific heat C measured at different magnetic fields for CaRuO_3 , $\text{Sr}_{0.1}\text{Ca}_{0.9}\text{RuO}_3$, and $\text{Sr}_{0.2}\text{Ca}_{0.8}\text{RuO}_3$. The solid red lines indicate the regions of LFL behaviour. Inset: Magnetic field dependence of C for CaRuO_3 at 0.5 K.

temperature scale, are shown for all investigated compounds in Fig. 4. At first, one should notice as a general feature that the most distinct increase of C/T dependence to the lowest accessible temperatures take place not in zero but in very weak critical magnetic fields which amount to approximately $B_0 \simeq 0.27(2) \text{ T}$ in CaRuO_3 and $\text{Sr}_{0.1}\text{Ca}_{0.9}\text{RuO}_3$ and $B_0 \simeq 0.20(2) \text{ T}$ in $\text{Sr}_{0.2}\text{Ca}_{0.8}\text{RuO}_3$. The values of these critical fields could be identified from the magnetic field dependence of C/T at 0.5 K which have the distinct maxima at B_0 shown for the $x = 1.0$ compound in the insert in Fig. 4. In the magnetic fields which are lower (in our case it is only $B = 0$) or higher than these critical values the LFL properties are well seen and one can notice a gradual increase of the regions of the Fermi liquid behaviour with increasing field. In $\text{Sr}_{0.2}\text{Ca}_{0.8}\text{RuO}_3$ the temperature dependence of C/T shows the distinct increase to the lowest temperatures in the field of 0.2 T. These anomalous increase of the C/T ratio in the weak magnetic fields are discussed separately.

The values of T_{LFL} derived from the upper limit of the $C/T = \text{const}$ behaviour were used to prepare the low

temperature part of the phase diagrams which separate regions with LFL and NFL behaviour on the T - B plane (Fig. 7). The numerical values of T_{LFL} are gathered in Table I in the Supplemental materials.

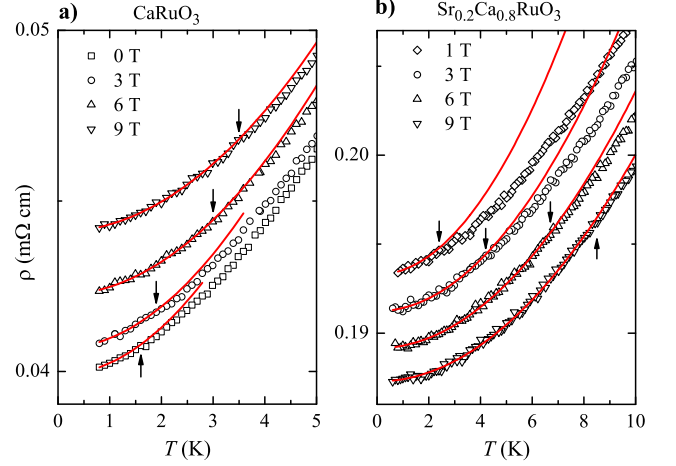


FIG. 5: (Color online) Resistivity of a) CaRuO_3 and b) $\text{Sr}_{0.2}\text{Ca}_{0.8}\text{RuO}_3$ measured at different magnetic fields. The curves in b) are shifted by a multiplication of $0.002 \text{ m}\Omega \cdot \text{cm}$ for clarity. Solid lines were fitted using the T^2 law. Arrows mark the temperature T_{LFL} where T^2 law starts to deviate from experimental data.

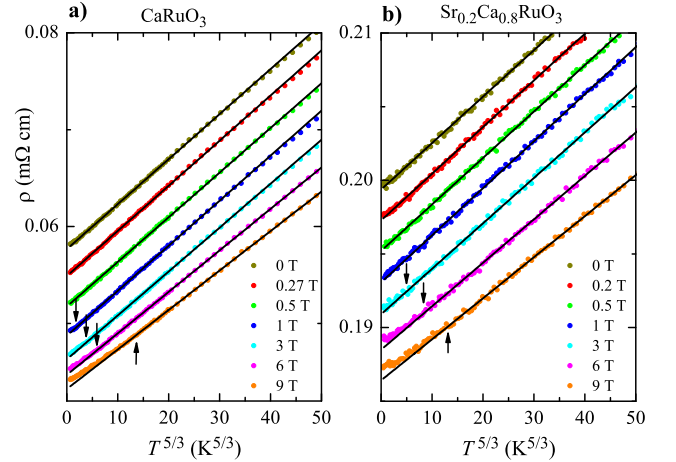


FIG. 6: (Color online) Resistivity of a) CaRuO_3 and b) $\text{Sr}_{0.2}\text{Ca}_{0.8}\text{RuO}_3$ measured at different magnetic fields. For clarity, the curves in a) and b) are shifted by a multiplication of 0.003 and $0.002 \text{ m}\Omega \cdot \text{cm}$, respectively. Solid lines were fitted using the $T^{5/3}$ law. Arrows mark the lower limit of the region where this law well reproduces experimental data.

The distinct NFL properties above T_{LFL} and the gradual increase of the range of LFL behaviour in higher fields are corroborated by the results of the resistivity measurements. The temperature evolution of the electrical resistivity for CaRuO_3 and $\text{Sr}_{0.2}\text{Ca}_{0.8}\text{RuO}_3$ are shown in Fig. 5 and 6. It can be notice that at low temperatures

the resistivity for each compound demonstrate the LFL temperature dependence (Fig. 5a and 5b). The least-squares analysis using the formula $\rho(T) = \rho_0 + a_2 T^2$ allow to determine the residual resistivity ρ_0 , the field dependent $a_2(B)$ coefficients and to derive the T_{LFL} temperatures from the upper limit of T^2 behaviour. As it was already mentioned, because of the limited accuracy of our measurements such analysis can only be performed when T_{LFL} values exceed approximately 2 K. Fortunately, in the strong magnetic fields range of the Fermi liquid behaviour distinctly grows up and even exceeds 8 K for the $x = 0.8$ compound in the field of 9 T. The values of T_{LFL} derived from the resistivity measurements establish the high temperature part of the LFL/NFL phase diagram shown in Fig. 7. In Fig. 8 it was proved that the variation of $a_2(B)$ coefficients with the magnetic fields obtained from the data for $B \geq 3$ T fulfil the relation $a_2(B) \sim (B - B_0)^{-1}$.⁵⁰ All numerical values of ρ_0 , a_2 and T_{LFL} are collected in Table II in the Supplemental material.

As in the zero magnetic field, above the Landau Fermi liquid temperatures T_{LFL} all investigated materials show the NFL behaviour characterized by the increase of C/T with decreasing temperature and $T^{5/3}$ dependence of the electrical resistivity. The temperature variations of $\rho(T)$ for CaRuO_3 and $\text{Sr}_{0.2}\text{Ca}_{0.8}\text{RuO}_3$ in different magnetic fields are shown in Fig. 6a and 6b. The continuous lines represent the results of the least-squares analysis using the formula $\rho(T) = \rho_0^* + a_{5/3} T^{5/3}$. One can note that in the fields B_0 (or close to B_0) the NFL relation $\rho(T) \sim T^{5/3}$ very well describe the experimental data in all investigated compounds to the lowest accessible temperatures. It should be also remarked that at or close to B_0 this NFL formula very well describe the experimental data over one decade of temperature. The numerical values of the fitted parameters (ρ_0^* and $a_{5/3}$ as well as the ranges of application of this description which are shown in some drawings by arrows, are given for CaRuO_3 and $\text{Sr}_{0.2}\text{Ca}_{0.8}\text{RuO}_3$ in Table II in the Supplemental materials.

IV. COMPARISON WITH THEORETICAL MODELS. DISCUSSION.

In part A of this section, the experimental results of the specific heat and electrical resistivity are compared with predictions of the Moriya's self-consistent renormalization theory (SCR) of spin fluctuations.^{42,46} The C/T temperature dependences with subtracted lattice contributions $(C/T)_{lat}$ were least-squares fitted using the appropriate SCR formulas for the 3-dimensional ferromagnetic materials⁴⁶ and the phenomenological parameters which characterize the spectrum of spin fluctuations were determined. Then, these parameters were used to analyse the temperature dependence of the resistivity $\rho(T)$. More details about the whole procedure are given in the appropriate subsection. The procedure of the calculation

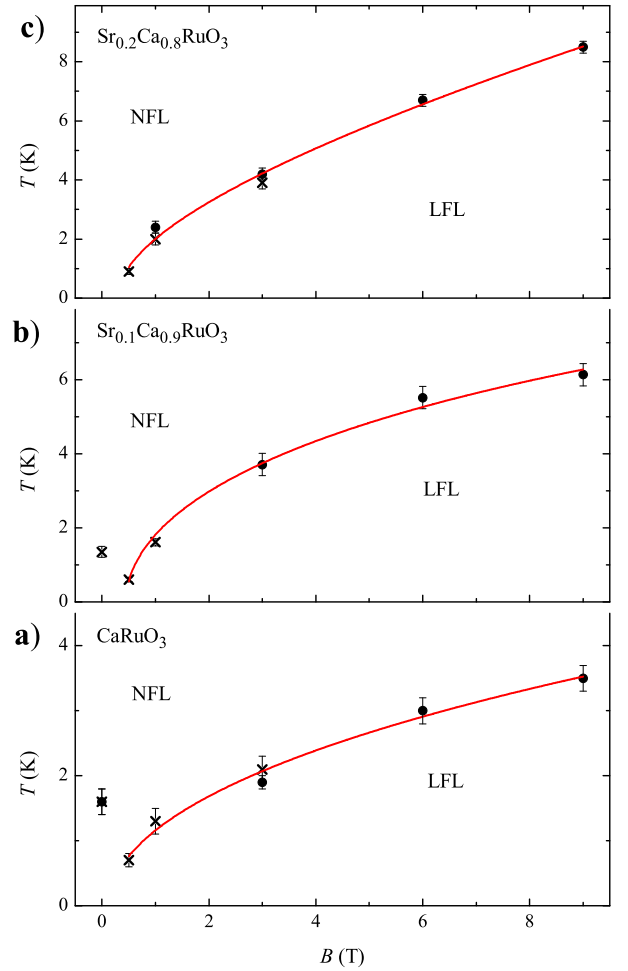


FIG. 7: T - B phase diagrams of $\text{Sr}_{1-x}\text{Ca}_x\text{RuO}_3$ for $x = 0.8$, 0.9 , and 1.0 with the regions of Landau Fermi liquid (LFL) and non-Fermi liquid (NFL) regions. Points were obtained from analyses of resistivity data (dots) and specific heat (crosses). Solid lines are drawn to guide the eye.

of the lattice contribution $(C/T)_{lat}$ is also discussed. In part B, the temperature dependences of the electrical resistivity for all investigated compounds and in all applied magnetic fields were analysed within the ‘hidden Fermi liquid’ theory of Anderson.⁴⁸

A. Specific heat and resistivity within the SCR theory of spin fluctuations

At the beginning, the self-consistent renormalization (SCR) theory of spin fluctuations developed mostly by Moriya has been successfully applied to describe the magnetic and thermodynamics properties of the nearly and weakly ferro- and antiferromagnetic metallic systems.^{42,43} Then, this theoretical approach was extended to analyse the non-Fermi liquid behaviour of the specific heat and electrical resistivity of the antiferromagnetic heavy electron systems in the region of enhanced

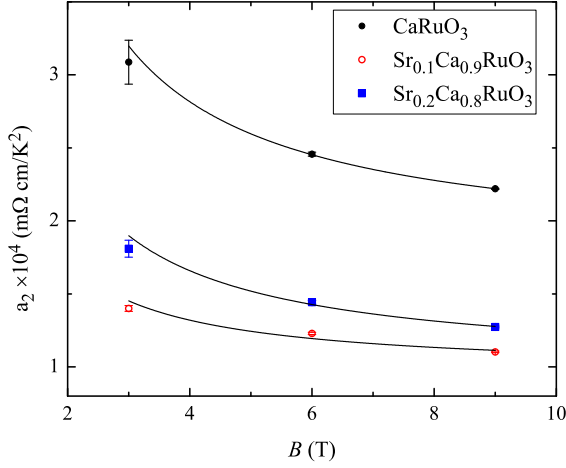


FIG. 8: Coefficient a_2 of the T^2 law of the resistivity, determined for $\text{Sr}_{1-x}\text{Ca}_x\text{RuO}_3$ for $x = 0.8, 0.9$, and 1.0 in the Landau Fermi liquid phase.

spin-fluctuations near the magnetic instability.⁴⁷ In particular, the temperature dependence the specific heat and electrical resistivity were calculated and compare with the experimental data.^{45,47} Simultaneously, the theory was applied in the analysis of the anomalous non-Fermi liquid behaviour of the specific heat close to the magnetic instability in the itinerant ferromagnets and to detailed discussion of the crossover between LFL and NFL properties.⁴⁶

In the SCR theory of spin fluctuations the imaginary part of the low frequency ω and long wave-length q -dependent dynamic magnetic susceptibility $\chi(\omega, q)$ is parametrized by two energy scales T_0 and T_A which characterize the energy width of the spin fluctuation spectrum and the dispersion of the wave-vector dependent static susceptibility in the q -space, respectively. In addition, two dimensionless parameters were introduced: y_0 which is a zero temperature inverse magnetic susceptibility and measures the proximity to the magnetic instability and y_1 which reflects the strength of the coupling between the fluctuations with different wave-vector (mode-mode coupling). These four phenomenological parameters which can be experimentally determined from the bulk magnetic and neutron scattering experiments allow within the SCR theory to analyse the magnetic, thermodynamic and transport properties. All physical quantities can be derived from the reduced inverse magnetic susceptibility $y = 1/(T_A \chi_Q(0))$ (Q is the antiferromagnetic order wave-vector, for the ferromagnet $Q = 0$) which can be determined by solution of the following integral self-consistent equation

$$y = y_0 + \frac{3}{2}y_1 \int_0^1 dx x^3 \left[\ln u - \frac{1}{2u} - \psi(u) \right] \quad (1)$$

where

$$u = \frac{x(y + x^2)}{t}, \quad t = T/T_0, \quad (1a)$$

and $\psi(u)$ denotes the digamma function.

The temperature dependence of the molar specific heat caused by excitations of the spin fluctuations is given by the formula⁴⁶

$$C_m = 9N_0k_B \int_0^1 dx x^2 \left\{ \left[u^2 - 2ux \frac{dy}{dx} + x^2 \left(\frac{dy}{dx} \right)^2 \right] \cdot \left[-\frac{1}{u} - \frac{1}{2u^2} - \psi'(u) \right] - tx \frac{d^2y}{dt^2} \left[\ln u - \frac{1}{2u} - \psi(u) \right] \right\} \quad (2)$$

where N_0 is the Avogadro number, k_B is the Boltzmann constant, $\psi'(u)$ denotes the trigamma function and the other parameters have the same meaning as in Eq. (1). The low temperature limit of Eq. (2) has the form

$$\frac{C_m}{T} = \frac{3N_0k_B}{4T_0} \left[\ln \left(1 + \frac{1}{y_0} \right) - \frac{2t^2}{5y_0^3} \ln \left(\frac{y_0}{t} \right) + O(t^2) \right], \quad \text{for } y_0 > 0, \quad (2a)$$

with the saturation value at zero temperature $(3N_0k_B/4T_0) \ln(1 + 1/y_0)$. The temperature dependence at the critical phase boundary is described by the formula

$$\frac{C_m}{T} = \frac{N_0k_B}{2T_0} \ln(1/t), \quad \text{for } y_0 = 0. \quad (2b)$$

This logarithmic behaviour should be observed at low temperatures close to the magnetic instability.

The temperature dependence of the electrical resistivity for the 3-dimensional metal caused by scattering of conduction electrons by the ferromagnetic SF is given, within the SCR theory, by the formula⁴²

$$R(T) = r\bar{R}(T), \quad (3)$$

where the temperature independent coefficient r allows to distinguish between FM and AFM metals. The whole temperature dependence is contained in the $\bar{R}(T)$ factor which in the case of 3-dimensional ferromagnetic metal has the form

$$\bar{R}(T) = 3 \int_0^1 dx x^4 \left[-1 - \frac{1}{2u} + u\psi'(u) \right]. \quad (4)$$

As in the case of the specific heat calculations the reduced magnetic susceptibility y has to be numerically calculated from Eq. (1). At the very low temperatures the resistivity is described by the LFL formula $\rho \sim T^2$ and at the critical boundary ($y_0 = 0$) and in the NFL region one gets⁴²

$$\bar{R}(T) = 0.9385 t^{5/3}. \quad (4a)$$

Our experimental specific heat and electrical resistivity of $\text{Sr}_{1-x}\text{Ca}_x\text{RuO}_3$ qualitatively follow the theoretical predictions. At low temperatures the specific heat show in general the $C/T = \text{const}$ behaviour characteristic for the

Fermi liquid and at higher temperatures a monotonous pseudo-logarithmic decrease of C/T with increasing temperature is observed. The qualitative agreement with the theoretical predictions appears also for the experimental results of the electrical resistivity. At low temperatures characteristic for the LFL $\rho \sim T^2$ behaviour is observed whereas above T_{LFL} the NFL variation $\rho(T) \sim T^{5/3}$ is observed.

In the quantitative analysis one should take into account that the total experimentally determined specific heat is the sum of several contributions

$$\frac{C}{T} = \gamma_0 + \frac{C_m}{T} + \frac{C_{lat}}{T}, \quad (5)$$

where except the spin fluctuations part C_m , C_{lat} denotes the lattice contribution and γ_0 represents the electronic specific heat coefficient which results from the finite density of states at the Fermi energy.

The numerical analysis of the specific heat within the SCR theory should in principle give a proper description of the C/T behaviour and allow to determine the phenomenological SCR parameters y_0 , y_1 and T_0 was rather complicated and will be described in the following in a few steps. At the beginning of the discussion we concentrate on pure CaRuO_3 in zero magnetic field where the situation is the most clear. Then, the analysis is extended to specific heat behaviour in external magnetic field and for solid solutions with different strontium concentration.

Since the NFL anomaly in the temperature dependence of the specific heat is very small (increase of C/T ratio below 10 K is below $10 \text{ mJ mol}^{-1} \text{K}^{-2}$) it is very important to get independently the reliable temperature dependence of the lattice contribution. The lattice contribution for CaRuO_3 used in calculations in this work was obtained from the experimentally determined specific heat of CaRhO_3 scaled by the procedure proposed in Ref. 54. CaRhO_3 is a metallic paramagnet at least down to 2 K. The temperature dependence of C/T below 20 K does not show any anomalies and can be described as a sum of the electronic and lattice contributions.⁵¹ The experimental data presented as C/T vs T^2 are shown in Fig. 9. This behaviour was parametrized using the Debye and Einstein models of the lattice specific heat. Such parametrization of C_{lat} should be very useful in the analysis of the lattice contributions in the solid solutions where the calcium atoms are replaced by the heavier strontium and no suitable analogs with rhodium compounds exist.

The detailed numerical analysis of the CaRhO_3 specific heat proves the linear variation of C/T vs T^2 below approximately 10 K and in this range of temperatures the Debye model is enough to describe the specific heat behaviour and the linear fit allows to determine the Debye temperature Θ_D (Fig. 9, inset). To get a satisfactory description of C_{lat} above 10 K one has to add a small additional contribution which reflects an excitation of optical phonons and is taken into account within the Einstein model of the specific heat. It was found

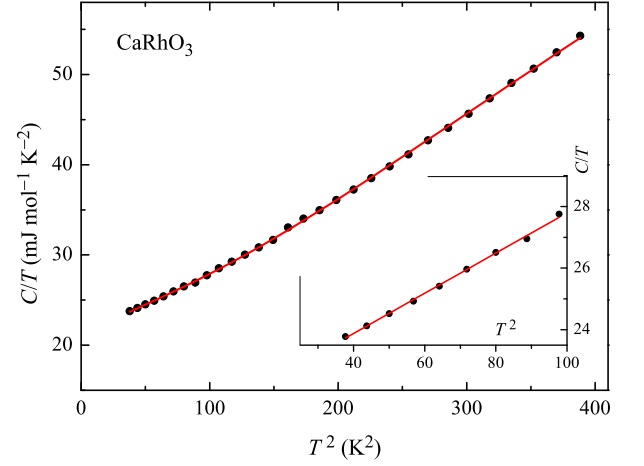


FIG. 9: Specific heat of CaRhO_3 (based on Ref. 51) analyzed within the Debye and Einstein models of the lattice specific heat.

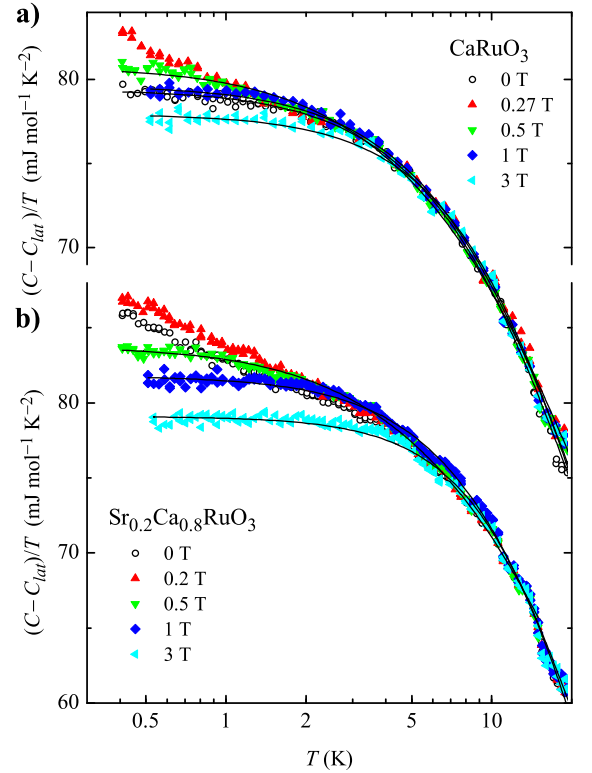


FIG. 10: (Color online) Specific heat after subtracting the lattice contribution $C - C_{lat}$ for CaRuO_3 and $\text{Sr}_{0.2}\text{Ca}_{0.8}\text{RuO}_3$ at different magnetic fields. The solid lines were fitted using the SCR model of spin fluctuations (see text).

that one frequency parametrized as an Einstein temperature Θ_E is enough to get the very good description of C_{lat} in the range of temperatures up to 20 K. The fitted function which contains both contributions is shown as a continuous line in the main panel of Fig. 9. The following values of the parameters were determined from the

least-squares analysis: $\Theta_D = 530(3)$ K, $\Theta_E = 117(3)$ K and $\gamma_0(\text{CaRuO}_3) = 21.3(1)$ mJ·mol⁻¹·K⁻². The amount of the Einstein contribution to the total specific heat is approximately 1.3%. After the atoms mass scaling to CaRuO₃ the characteristic temperatures amount $\Theta_D = 533.0$ K and $\Theta_E = 117.8$ K. As a final important remark concerning the lattice specific heat one should notice that C_{lat} is completely negligible below approximately 2.2 K, so below this temperature the experimental specific heat contains only the electronic and the spin-fluctuations contributions.

After subtraction of the lattice contribution, the specific heat depends on four parameters: the electronic contribution γ_0 and the three parameters which describe the spin-fluctuation contribution within the SCR Moriya's theory: y_0 , y_1 and T_0 . In principle, these parameters could be determined simultaneously using the least-squares fitting procedure. Nevertheless, a correlation between the parameters in connection with the rather smooth experimental C/T curves make the least-squares calculations very unstable, for example it is difficult to obtain expected smooth variation of fitted parameters with increasing magnetic field. More reliable analysis of the C/T behaviour needs reduction of the number of independently varied parameters. The procedure which we used is described below. As in the case of determination of C_{lat} , the discussion concentrates on pure CaRuO₃ in zero field and the rules are later applied in the analysis of the specific heat for the other compounds in different magnetic fields.

First of all, the electronic contribution γ_0 was determined independently and constrained in the further minimization procedure. It was calculated by the analysis of the lowest part of the C/T dependence taking into account a correction to the description within the Landau Fermi liquid theory caused by the spin-fluctuations. The suitable formula which contains the $-T^3 \log T$ contribution to the specific heat, was obtained within the paramagnon theory by many authors (they are mentioned in the quoted reference) and the most convenient form for our purpose is given as⁵²

$$\frac{C}{T} = \gamma_0 \left[\frac{m^*}{m} + \alpha_0 \left(\frac{T}{T_{sf}} \right)^2 \ln \left(\frac{T}{T_{sf}} \right) \right] \quad (6)$$

where m^*/m denotes the mass enhancement factor, T_{sf} is the spin-fluctuation temperature and α_0 can be expressed by the Stoner enhancement factor.

This formula well describes the C/T ratio even in the wide range of temperatures but the values of α_0 and T_{sf} strongly depend on the temperature range taken into account in the minimization procedure. Nevertheless, γ_0 and m^*/m which are varied as independent parameters do not vary much and for CaRuO₃ in zero magnetic field $\gamma_0 \simeq 10.0(2)$ mJ·mol⁻¹·K⁻² and $m^*/m \simeq 7.9(2)$. Since the temperature dependent factor in formula (6) disappears at zero temperature, the product $\gamma_0(m^*/m)$ is equal to the C/T ratio extrapolated to zero Kelvins which

for CaRuO₃ at zero field amounts to $\simeq 79.3$ mJ/molK². The values of γ_0 and m^*/m can be compared with the theoretical predictions. Theoretically calculated value of the electronic contribution was reported to be equal to $\gamma_0 \simeq 9.54$ mJ/molK².²² In addition, the detailed theoretical calculations of the electronic structure of SrRuO₃ and CaRuO₃ were recently reported.⁵³ Since the values of the mass enhancement factors were calculated for different values of an effective onsite interactions U and a Hund's couplings J , it is not possible to have a direct comparison with the result of our analysis. Nevertheless, our $m^*/m \simeq 7.9(2)$ is in the range of the calculated values in some regions of U and J parameters.

Finally, in the first step of the analysis the relation between the spin-fluctuations contribution to the specific heat and the Moriya's parameters at zero kelvins: $(C_m/T)_{T=0} = (3N_0 k_B / 4T_0) \ln(1 + 1/y_0)$ was used. Since $(C_m/T + \gamma_0)$ can be directly determined from the experimental data as the average values of C/T in the flat LFL region and with known electronic contribution γ_0 one can express T_0 by y_0 and use only two parameters as independent variables in the least-squares analysis: y_0 and y_1 . In the last step, when the values of y_0 , y_1 and T_0 were in the proper region of the parameters space, all 3 SCR parameters were allowed to vary giving the final solution.

Since the described analysis of the electronic and lattice contributions concerned only CaRuO₃ at zero magnetic field one has to transfer some rules of analysis to compounds with different compositions and in the different external magnetic fields.

In order to analyse the specific heat behaviour in different magnetic fields it was assumed that the electronic and the lattice contributions do not vary with field. The field independence of C_{lat} can be inferred from the observation that the experimental C/T values above 15 K where the lattice contribution is dominant over the electronic and spin-fluctuations contributions practically do not depend on the magnetic field. Then, the zero temperature values of C/T which are given by the product $\gamma_0(m^*/m)$ (see Eq. (6)) do not depend strongly on the magnetic field which means that one should not expect any serious variation of the electronic contribution with field. Indeed, the least-squares analysis of the low temperature C/T behaviours using Eq. (6) shows for each composition practically field independent values of γ_0 . All of that means that at low temperatures mostly the spin-fluctuations contribution is responsible for the observed variation of the specific heat with field.

As concerns the analysis of the specific heat for compounds with different calcium concentration, the zero field C/T behaviour shown in Fig. 1 announces serious differences in the lattice contributions. Since as it was already mentioned it would be not convenient to determine simultaneously all parameters which determine the electronic, lattice and spin-fluctuations contributions the analysis was performed in a few steps. At first, the least-squares analysis of the low temperature behaviour us-

ing Eq. (6) shows for each composition practically the same values of $\gamma_0 \simeq 10.0(2)$ mJ/molK². Then, observation that up to approximately 10 K the lattice dynamics is well described by the Debye model, the Debye temperature Θ_D with the SCR parameters and constrained $(C/T)_{T=0}$ was calculated by the least-squares analysis of the C/T at low temperatures. In the last step, y_0 , y_1 (T_0 calculated from constrained $(C/T)_{T=0}$) and two additional C_{lat} parameters (the Einstein temperature Θ_E and the Einstein contribution to the total specific heat) were calculated with constrained γ_0 and Θ_D from the all experimental points up to 20 K. The calculations were performed for the C/T temperature dependences for $x = 0.9$ and 0.8 materials in the field 1 T, which show already well developed LFL region. Finally, it was assumed that as in the case of CaRuO_3 for the mixed compounds C_{lat} and γ_0 do not depend on the magnetic field.

As a rule, only the C/T functions with subtracted lattice contributions were least-squares fitted within the SCR model using Eq. (2). The dimensionless inversed magnetic susceptibility $y(T)$ was obtained by numerical solution of Eq. (1) in a self-consistent way. The results of these calculations for CaRuO_3 and $\text{Sr}_{0.2}\text{Ca}_{0.8}\text{RuO}_3$ are shown by the continuous lines in Fig. 10. In general, quite good agreement between the experimental data and the theoretical curves was obtained for C/T behaviour at $B = 0$ (except of $x = 0.2$ sample) and fields $B \geq 0.5$ T. The results for $\text{Sr}_{0.1}\text{Ca}_{0.9}\text{RuO}_3$ in majority place between results for $x = 0.8$ and 1.0 compounds. The field dependences of the obtained SCR parameters for different compounds and different magnetic fields are shown in Fig. 13. The numerical values of y_0 , y_1 and T_0 were gathered in Table I in the Supplemental materials.

Temperature dependences of the specific heat for all materials in weak external magnetic fields (0.2–0.3 T) where the C/T ratio increases to the lowest accessible temperatures need some additional discussion. It was found that the increase in C/T values as a function of temperature and the maxima in their field dependence can be well described as a Schottky anomaly caused by the ferromagnetic clusters which in the external (or internal for $x = 0.2$ sample in $B = 0$) field behave as a two level system. The possibility of the existence of small magnetic clusters which can form at low temperatures the cluster glass state can be inferred from the results of the bulk magnetic measurements (difference between FC and ZFC susceptibilities in the weak magnetic fields and the hysteresis loop at 2 K) as well as from information delivered by the magnetic transition measurements²⁵ and the inelastic neutron scattering.⁵³ This cluster glass picture allowed for the quantitative description of the C/T behaviour as a function of temperature and magnetic field below approximately 2 K.

In addition, the temperature dependences of the electrical resistivity for all investigated compounds in different magnetic fields were analysed within the SCR spin fluctuations theory using the formulas (3) and (4). As

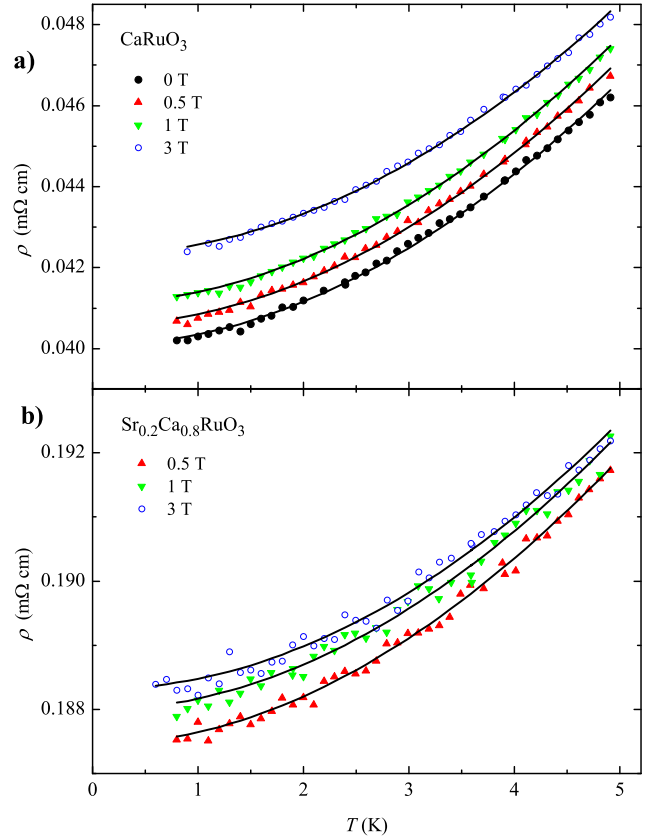


FIG. 11: (Color online) Resistivity of a) CaRuO_3 and b) $\text{Sr}_{0.2}\text{Ca}_{0.8}\text{RuO}_3$ measured at different magnetic fields. The curves in a) and b) are shifted by a multiplication of 0.0005 m Ω ·cm for clarity. The solid lines were fitted using the SCR model of spin fluctuations.

in the case of the specific heat analysis the dimensionless inverse magnetic susceptibility $y(T)$ was calculated from Eq. (1). Only the r parameter and the residual resistivity ρ_0 (not included in Eq. (3)) were chosen as the variable parameters in the least-squares procedure whereas the values of the SCR parameters y_0 , y_1 and T_0 were constrained to those obtained from the specific heat analysis. The results of these calculations are shown by the continuous lines in Fig. 11. The analysis shows that quite good agreement between the experimental data and theoretical description can be obtained up to approximately 5 K.

B. Resistivity and the ‘hidden Fermi liquid’ theory of Anderson

A different approach to the problem of NFL behaviour of the electrical resistivity in strongly correlated systems was developed by P. W. Anderson.⁴⁸ The aim of his ‘hidden Fermi liquid’ (HFL) theory was the explanation of the anomalous electron transport in the normal state of the high- T_C cuprate superconductors where the electri-

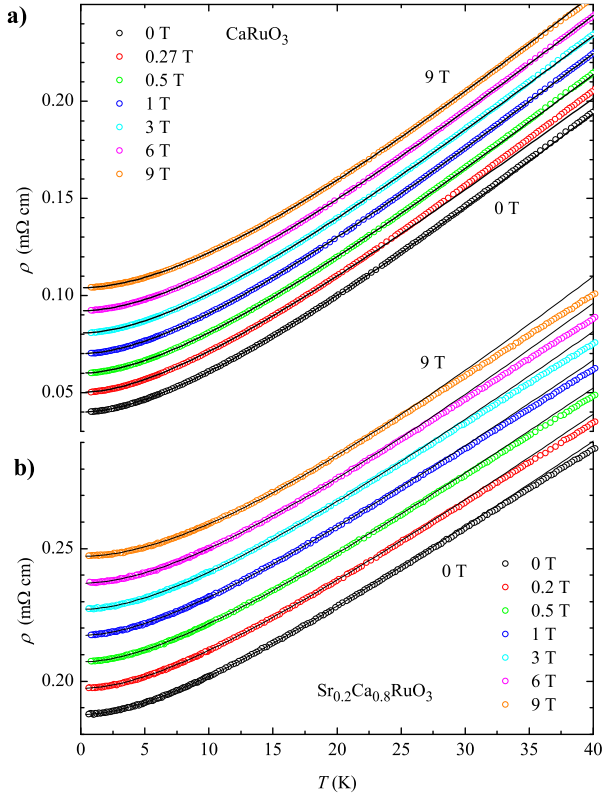


FIG. 12: (Color online) Resistivity of a) CaRuO_3 and b) $\text{Sr}_{0.2}\text{Ca}_{0.8}\text{RuO}_3$ measured at different magnetic fields. The curves in a) and b) are shifted by a multiplication of 0.01 mΩ cm for clarity. Solid black lines were fitted using the 'hidden Fermi liquid' model of Anderson.

cal resistivity varies from the linear T dependence in the optimally doped region to the LFL behaviour in the overdoped region. In the HFL theory the temperature dependence of the electrical resistivity is described by the following formula

$$\rho(T) = \rho_0 + a_A \frac{T^2}{T + W_{HFL}}, \quad (7)$$

where a prefactor $a_A = \hbar/(e^2 E_F)$ and W_{HFL} represents the HFL bandwidth connected with the quasi-particles scattering rate which can be probed by the angle-resolved photoemission spectroscopy (ARPES).

All the experimental ρ data were analysed using formula (7). In the least-squares procedure the residual resistivity ρ_0 , a_A prefactor and the W_{HFL} quasi-particles band-width were varied as independent parameters. The results of this analysis for CaRuO_3 and $\text{Sr}_{0.2}\text{Ca}_{0.8}\text{RuO}_3$ are shown in Fig. 12. It can be concluded, that Eq. (7) assures quite good description of the $\rho(T)$ behaviour for the investigated compounds in the wide range of magnetic fields up to approximately 25 K. There is only a very weak field dependence of the a_A prefactor which seems to be justified by the formula shown below Eq. (7). On the contrary, the HFL bandwidth considerably increases

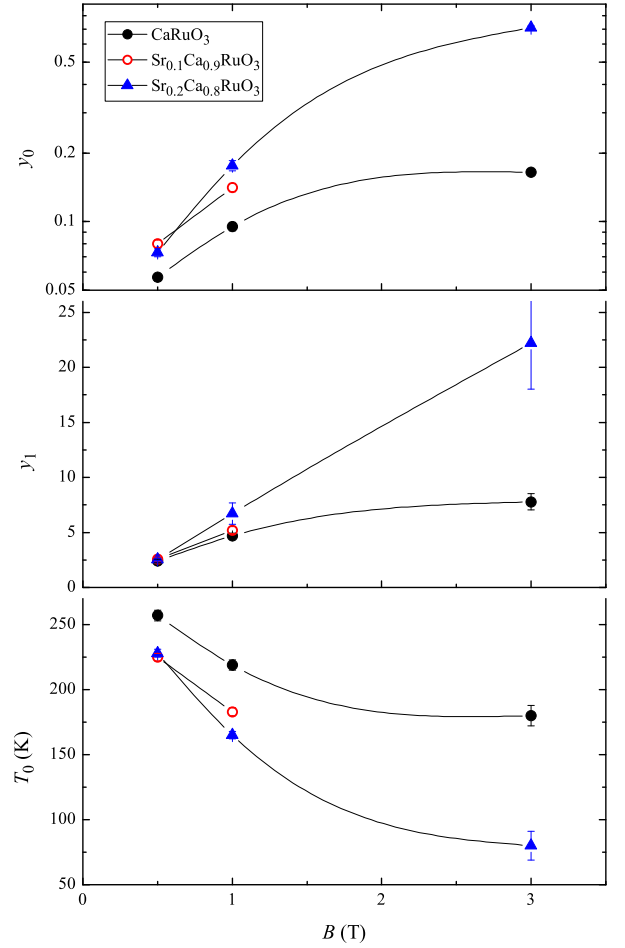


FIG. 13: Magnetic field dependence of the SCR parameters determined from fitting specific heat data for $\text{Sr}_{1-x}\text{Ca}_x\text{RuO}_3$ for $x = 0.8, 0.9$, and 1.0 . The solid lines are to guide the eye.

with rising magnetic field (it increases even by a factor of two for $\text{Sr}_{0.2}\text{Ca}_{0.8}\text{RuO}_3$ in the field of 9 T), it means for the materials with increasing LFL character. It seems to be in consent with distinct increase of the W_{HFL} values in the $\text{La}_{2-x}\text{Sr}_x\text{CuO}_4$ high- T_C superconductor with increase of the strontium concentration when the system develops from the NFL to the LFL behaviour in the overdoped region.

V. SHORT SUMMARY

In this paper we report the results of the specific heat and the resistivity measurements for $\text{Sr}_{1-x}\text{Ca}_x\text{RuO}_3$ compounds with the calcium concentration $x \geq 0.8$. The measurements were performed in the wide range of temperatures and external magnetic fields. In the indicated range of concentrations the materials show the anomalous properties which do not agree with predictions of the Landau Fermi liquid theory. Careful analysis of the C/T and $\rho(T)$ behaviour allowed to determine the

Landau Fermi liquid temperature which separates the Fermi liquid region ($C/T = \text{const}$ and $\rho \sim T^2$) from the region of the anomalous non Fermi liquid behaviour identified by the $\rho \sim T^{5/3}$ temperature dependence of the resistivity and prepare the T - x and T - B phase diagrams for the investigated materials. In addition, the experimental results were compared with predictions of the self-consistent renormalization theory of spin fluctuations of Moriya (specific heat and resistivity) and with the ‘hidden Fermi liquid’ theory of Anderson (resistivity). Rather good agreement was found between the experimentally determined and theoretically calculated behaviour in some ranges of temperature. Detected anomalous increase of C/T below approximately 2 K for all investigated materials at very low magnetic fields of 0.2–0.3 T (at zero field for the $x = 0.2$ sample) was inter-

preted as caused by the Schottky type anomaly induced by the ferromagnetic clusters.

Acknowledgments

This work was financed by the Polish National Science Centre within research project DEC-2011/01/B/ST3/00436. Measurements were carried out with the equipment purchased thanks to the financial support of the European Regional Development Fund in the framework of the Polish Innovation Economy Operational Program (contract no. POIG.02.01.00-12-023/08). We thank Prof. K. Yamaura for providing us the numerical data of CaRhO_3 specific heat.

- ¹ H. v. Löhneysen, A. Rosch, M. Vojta, and P. Wölfle, *Rev. Mod. Phys.* **79**, 1015 (2007).
- ² K. Kadowaki, S. B. Woods, *Solid State Commun.* **58**, 507 (1986).
- ³ N. Tsujii, H. Kontani, and K. Yoshimura, *Phys. Rev. Lett.* **94**, 057201 (2005).
- ⁴ G. R. Stewart, *Rev. Mod. Phys.* **73**, 797 (2001); G. R. Stewart, *Rev. Mod. Phys.* **78**, 743 (2006).
- ⁵ M. Vojta, *Rep. Progr. Phys.* **66**, 2069 (2003).
- ⁶ H. v. Löhneysen, T. Pietrus, G. Portisch, H. G. Schlager, A. Schröder, M. Sieck, and T. Trappmann, *Phys. Rev. Lett.* **72**, 3262 (1994); B. Bogenberger and H. v. Löhneysen, *Phys. Rev. Lett.* **74**, 1016 (1995); H. v. Löhneysen, C. Pfleiderer, T. Pietrus, O. Stockert, and B. Will, *Phys. Rev. B* **63**, 134411 (2001).
- ⁷ O. Trovarelli, C. Geibel, S. Mederle, C. Langhammer, F. M. Grosche, P. Gegenwart, M. Lang, G. Sparn, and F. Steglich, *Phys. Rev. Lett.* **85**, 626 (2000); P. Gegenwart, J. Custers, C. Geibel, K. Neumaier, T. Tayama, K. Tenya, O. Trovarelli, and F. Steglich, *Phys. Rev. Lett.* **89**, 056402 (2002).
- ⁸ C. Pfleiderer, G. J. McMullan, S. R. Julian, and G. G. Lonzarich, *Phys. Rev. B* **55**, 8330 (1997); C. Pfleiderer, S. R. Julian, and G. G. Lonzarich, *Nature* **414**, 427 (2001).
- ⁹ M. Uhlarz, C. Pfleiderer, and S. M. Hayden, *Phys. Rev. Lett.* **93**, 256404 (2004); M. Sutherland, R. P. Smith, N. Marcano, Y. Zou, S. E. Rowley, F. M. Grosche, N. Kimura, S. M. Hayden, S. Takashima, M. Nohara, and H. Takagi, *Phys. Rev. B* **85**, 035118 (2012).
- ¹⁰ P. G. Niklowitz, F. Beckers, G. G. Lonzarich, G. Knebel, B. Salce, J. Thomasson, N. Bernhoeft, D. Braithwaite, and J. Flouquet, *Phys. Rev. B* **72**, 024424 (2005).
- ¹¹ M. Nicklas, M. Brando, G. Knebel, F. Mayr, W. Trinkl, and A. Loidl, *Phys. Rev. Lett.* **82**, 4268 (1999); C. Franz, C. Pfleiderer, A. Neubauer, M. Schulz, B. Pedersen, and P. Böni, *J. Phys.: Conf. Ser.* **200**, 012036 (2010).
- ¹² D. A. Sokolov, M. C. Aronson, W. Gannon, and Z. Fisk, *Phys. Rev. Lett.* **96**, 116404 (2006).
- ¹³ J. Yang, B. Chen, H. Ohta, C. Michioka, K. Yoshimura, H. Wang, and M. Fang, *Phys. Rev. B* **83**, 134433 (2011).
- ¹⁴ M. Brando, D. Belitz, F. M. Grosche, and T. R. Kirkpatrick, *Rev. Mod. Phys.* **88**, 025006 (2016).
- ¹⁵ A. Kanbayasi, *J. Phys. Soc. Japan* **44**, 108 (1978).
- ¹⁶ G. Cao, S. McCall, M. Shepard, J. E. Crow, and R. P. Guertin, *Phys. Rev. B* **56**, 321 (1997).
- ¹⁷ T. Kiyama, K. Yoshimura, and K. Kosuge, in *Advances in Superconductivity IX*, edited by S. Nakajima and M. Murakami (Springer-Vorlag, Tokyo, 1997), p. 281.
- ¹⁸ K. Yoshimura, T. Imai, T. Kiyama, K. R. Thurber, A. W. Hunt, and K. Kosuge, *Phys. Rev. Lett.* **83**, 4397 (1998).
- ¹⁹ T. Kiyama, K. Yoshimura, K. Kosuge, H. Mitamura, and T. Goto, *J. Phys. Soc. Japan* **68**, 3372 (1999).
- ²⁰ D. Fuchs, C. L. Huang, J. Schmalian, M. Wissinger, S. Schuppler, K. Grube, and H. v. Löhneysen, *Eur. Phys. J. Special Topics* **224**, 1105 (2015); D. Fuchs, M. Wissinger, J. Schmalian, C.-L. Huang, R. Fromknecht, R. Schneider, and H. v. Löhneysen, *Phys. Rev. B* **89**, 174405 (2014).
- ²¹ Z. Fang and K. Terakura, *J. Phys.: Condens. Matter* **14**, 3001 (2002).
- ²² H. Mukuda, K. Ishida, Y. Kitaoka, K. Asayama, R. Kanno, and M. Tanaka, *Phys. Rev. B* **60**, 12279 (1999).
- ²³ A. Koriyama, M. Ishizaki, T. C. Ozawa, T. Taniguchi, Y. Nagata, H. Samata, Y. Kobayashi, Y. Noro, *J. Alloys Compd.* **372**, 58 (2004).
- ²⁴ M. Rams, R. Kmieć, J. Gurgul, Ż. Świątkowska, M. Kruzel, K. Król, and K. Tomala, *J. Alloys Compd.* **471**, 5 (2009).
- ²⁵ L. Demkó, S. Bordács, T. Vojta, D. Nosadze, F. Hrahsheh, C. Svoboda, B. Dóra, H. Yamada, M. Kawasaki, Y. Tokura, and I. Kézsmárki, *Phys. Rev. Lett.* **108**, 185701 (2012).
- ²⁶ Y. J. Uemura, T. Goko, I. M. Gat-Malureanu, J. P. Carlo, P. L. Russo, A. T. Savici, A. Aczel, G. J. MacDougall, J. A. Rodriguez, G. M. Luke, S. R. Dunsiger, A. McCollam, J. Arai, Ch. Pfleiderer, P. Böni, K. Yoshimura, E. Baggio-Saitovitch, M. B. Fontes, J. Larrea, Y. V. Sushko, and J. Sereni, *Nat. Phys.* **3**, 29 (2007).
- ²⁷ I. M. Gat-Malureanu, J. P. Carlo, T. Goko, A. Fukaya, T. Ito, P. P. Kyriakou, M. I. Larkin, G. M. Luke, P. L. Russo, A. T. Savici, C. R. Wiebe, K. Yoshimura, and Y. J. Uemura, *Phys. Rev. B* **84**, 224415 (2011).
- ²⁸ J. Gunasekera, L. Harriger, T. Heitmann, A. Dahal, H. Knoll, and D. K. Singh, *Phys. Rev. B* **91**, 241103(R) (2015).
- ²⁹ L. Capogna, A. P. McKenzie, R. S. Perry, S. A. Grigera, L.

- M. Galvin, P. Raychaudhuri, A. J. Schofield, C. S. Alexander, G. Cao, S. R. Julian, and Y. Maeno, *Phys. Rev. Lett.* **88**, 076602 (2002).
- ³⁰ P. Khalifah, I. Ohkubo, H. M. Christen, and D. G. Mandrus, *Phys. Rev. B* **70**, 134426 (2004).
- ³¹ P. B. Allen, H. Berger, O. Chauvet, L. Forro, T. Jarlborg, A. Junod, B. Revaz, and G. Santi, *Phys. Rev. B* **53**, 4393 (1996).
- ³² T. Kiyama, K. Yoshimura, K. Kosuge, H. Michor, and G. Hilscher, *J. Phys. Soc. Japan* **67**, 307 (1998).
- ³³ G. Cao, O. Korneta, S. Chikara, L. E. DeLong, and P. Schlottmann, *Solid State Comm.* **148**, 305 (2008).
- ³⁴ L. Klein, L. Antognazza, T. H. Geballe, M. R. Beasley, and A. Kapitulnik, *Phys. Rev. B* **60**, 1448 (1999).
- ³⁵ M. Schneider, D. Geiger, S. Esser, U. S. Pracht, C. Stingl, Y. Tokiwa, V. Moshnyaga, I. Sheikin, J. Mravlje, M. Scheffler, and P. Gegenwart, *Phys. Rev. Lett.* **112**, 206403 (2014).
- ³⁶ M. Schepard, S. McCall, G. Cao, and J. E. Crow, *J. Appl. Phys.* **81**, 4978 (1997).
- ³⁷ N. Kikugawa, L. Balicas, and A. P. Mckenzie, *J. Phys. Soc. Japan* **78**, 014701 (2009).
- ³⁸ A. Baran, A. Zorkovská, M. Kajňáková, J. Šebek, E. Santová, I. Bradarić, and A. Feher, *Phys. Status Solidi B* **249**, 1607 (2012).
- ³⁹ T. Vojta, *J. Low. Temp. Phys.* **161**, 299 (2010).
- ⁴⁰ J. A. Hertz, *Phys. Rev. B* **14**, 1165 (1976).
- ⁴¹ A. J. Millis, *Phys. Rev. B* **48** 7183 (1993).
- ⁴² T. Moriya, *Spin Fluctuations in Itinerant Electron Magnetism*, (Springer, Berlin, 1985); T. Moriya and K. Ueda, *Adv. Phys.* **49**, 555 (2000).
- ⁴³ T. Moriya and A. Kawabata, *J. Phys. Soc. Japan* **34**, 639 (1973); **35**, 669 (1973).
- ⁴⁴ G. G. Lonzarich and L. Taillefer, *J. Phys. C* **18**, 4339 (1985).
- ⁴⁵ S. Kambe, J. Flouquet, and T. H. Hargreaves, *J. Low. Temp. Phys.* **108**, 383 (1997).
- ⁴⁶ A. Ishigaki and T. Moriya, *J. Phys. Soc. Japan* **65**, 376 (1996).
- ⁴⁷ T. Moriya and T. Takimoto, *J. Phys. Soc. Japan* **64**, 960 (1995).
- ⁴⁸ P. W. Anderson, *Phys. Rev. B* **78**, 174505 (2008); P. W. Anderson and P. A. Casey, *Phys. Rev. B* **80**, 094508 (2009).
- ⁴⁹ Supplementary materials.
- ⁵⁰ P. Gegenwart, J. Custers, T. Tayama, K. Tenya, C. Geibel, O. Trovarelli, F. Steglich, and K. Neumaier, *Acta Phys. Pol. B* **34**, 323 (2003).
- ⁵¹ K. Yamaura, Y. Shirako, H. Kojitani, M. Arai, D. P. Young, M. Akaogi, M. Nakashima, T. Katsumata, Y. Inaguma, and E. Takayama-Muromachi, *J. Am. Chem. Soc.* **131**, 2722 (2009); K. Yamaura, private communication (2016).
- ⁵² K. Ikeda, S. K. Dhar, M. Yoshizawa, and K. A. Gschneidner, *J. Magn. Magn. Mater.* **100**, 292 (1991).
- ⁵³ H. T. Dang, J. Mravlje, A. Georges, and A. J. Millis, *Phys. Rev. B* **91**, 195149 (2015).
- ⁵⁴ M. Bouvier, P. Lethuillier, and D. Schmitt, *Phys. Rev. B* **43**, 13137 (1991).
- ⁵⁵ Z. Świątkowska, M. Rams, R. Kmiec, J. Gurgul, and K. Tomala, to be published.

VI. SUPPLEMENTAL MATERIAL

A. Bulk magnetic properties of $\text{Sr}_{1-x}\text{Ca}_x\text{RuO}_3$ ($x \geq 0.6$)

The main purpose of the bulk magnetic investigations was to get information about the magnetic properties of $\text{Sr}_{1-x}\text{Ca}_x\text{RuO}_3$ compounds in the range of calcium concentration where $T = 0$ phase transition between an itinerant ferromagnet and a paramagnetic metal was expected. This critical concentration was obtained by extrapolation of the values of Curie temperatures $T_C(x)$ to 0 K as equal to $x_c \simeq 0.7$.^{15,18} Later on, the existence of inhomogeneous ferromagnetic states in some concentration range near x_c was discovered by μSR ^{26,27} and precise magnetisation measurements on compositionally inhomogeneous thin film.²⁵

Nevertheless, checking bulk magnetic properties for our samples is important to ensure that the samples used for thermodynamic and electronic transport investigations are of good quality. Then it is important to know exactly whether the materials behave as ferromagnets, independently if all Ru moments participate in the ordering or there are only ferromagnetic clusters embodied into the paramagnetic matrix, and in which materials there is the paramagnetic state without any ferromagnetic impurities.

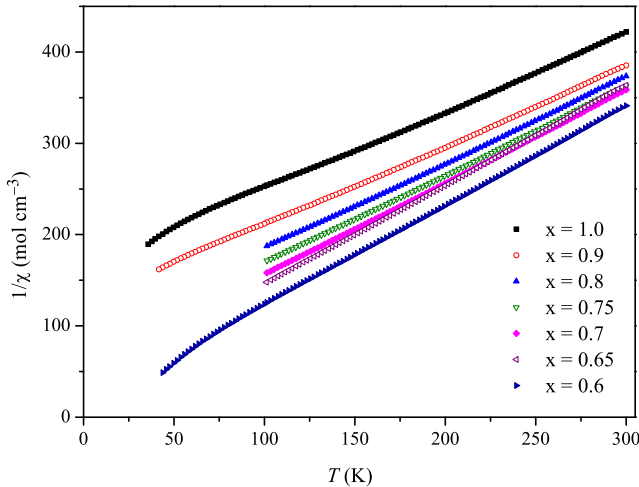


FIG. 14: Inverse of magnetic susceptibility measured at 1 kOe for the family of $\text{Sr}_{1-x}\text{Ca}_x\text{RuO}_3$ compounds.

The bulk magnetic measurements were performed on samples with calcium concentrations $x = 0.6, 0.65, 0.7, 0.75, 0.8, 0.9$ and 1.0 which cover the regions being on both sides of the critical concentration x_c . The investigations included the measurements of the ZFC and FC magnetic susceptibilities in weak magnetic field of 5 mT and a series of experiments sensitive to the ferromagnetic ordering which comprised: measurements of ac susceptibility $\chi'(T)$, search for the hysteresis loop at $T = 2$ K and the study of the magnetic equation of state (Arrott

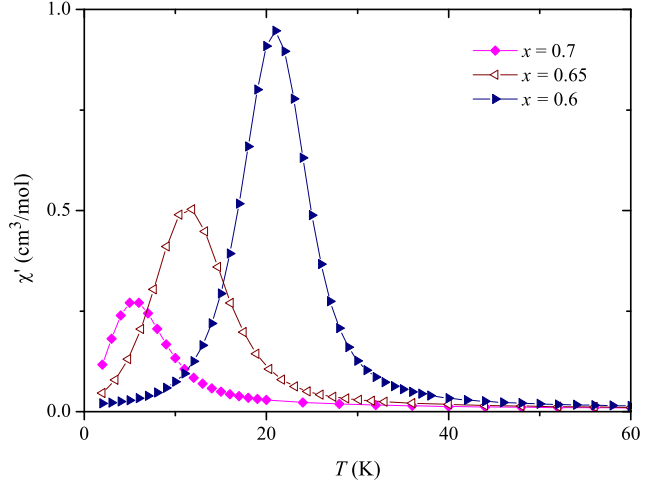


FIG. 15: Ac susceptibility measured at 3 Oe, 10 Hz showing ferromagnetic transitions for several $\text{Sr}_{1-x}\text{Ca}_x\text{RuO}_3$ samples.

plot).

Approximately above 100 K, the temperature dependence of the magnetic susceptibility for all the investigated materials are well described by the modified Curie-Weiss formula $\chi = \chi_0 + C/(T - \Theta_p)$, where C is a Curie constant, Θ_p denotes a paramagnetic Curie temperature and χ_0 contains all the temperature independent contributions to the magnetic susceptibility (Fig. 14). The paramagnetic Curie temperature Θ_p changes sign from positive to negative approximately at $x \simeq 0.6$. It can be also observed that values of the effective magnetic moments μ_{eff} inferred from the values of the molar Curie constants $C = N_0\mu_{eff}^2/(3k_B)$, where N_0 is the Avogadro number and k_B is the Boltzmann constant, practically do not vary with concentration being very close to the value for the ferromagnetic SrRuO_3 $\mu_{eff} \simeq 2.8\mu_B$, which has probably much more localized character of the magnetic moments in the Ru site,^{18,19,55} and show only minor increase for the materials with the calcium concentrations above 0.8.

The $\text{Sr}_{1-x}\text{Ca}_x\text{RuO}_3$ compounds with the calcium concentrations $x = 0.6, 0.65$ and 0.70 behave as ferromagnets. This is demonstrated by the distinct maxima in the temperature dependence of the ac susceptibility (Fig. 15) and by the presence of the hysteresis loop at 2 K (Fig. 16). For materials with the calcium concentration above 0.70 the hysteresis loop changes the character being much more elongated and very narrow (Fig. 17). This is probably connected with a partial ordering when only some fraction of the sample or even only small clusters show the ferromagnetic behaviour. The narrow hysteresis loops at 2 K for the $x = 0.75$ and $x = 0.8$ compositions are shown in the inset of Fig. 17. Searching carefully the magnetization process one finds also some irreversibility for $x = 0.90$ material and for pure CaRuO_3 (not shown).

Different magnetic properties of $x = 0.6$ and $x = 0.8$ are demonstrated by the investigation of the magnetic

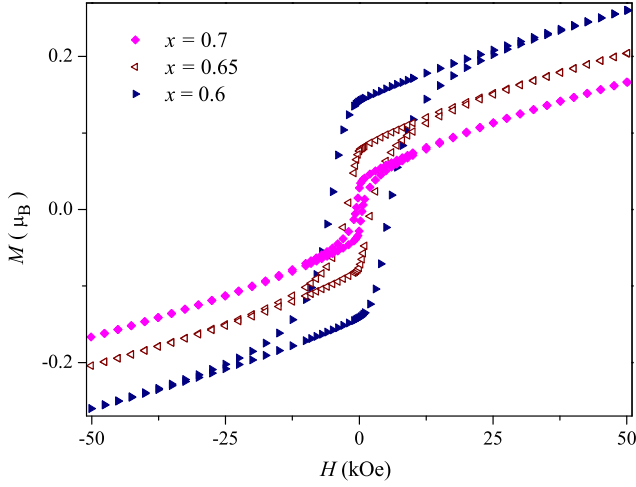


FIG. 16: Magnetic hysteresis loops for $\text{Sr}_{1-x}\text{Ca}_x\text{RuO}_3$ showing ferromagnetic phase.

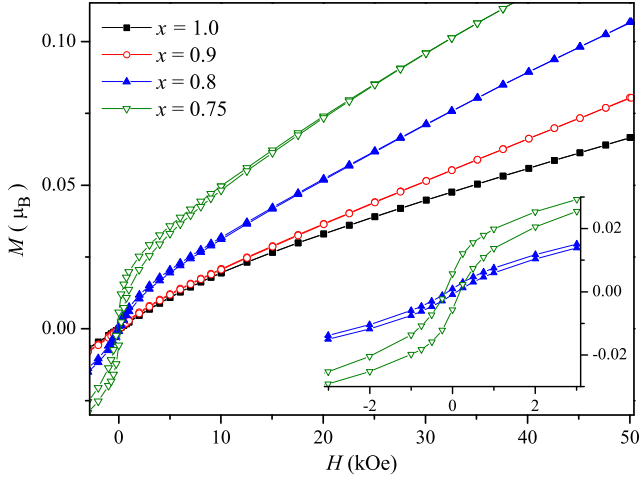


FIG. 17: Magnetic hysteresis loops for $\text{Sr}_{1-x}\text{Ca}_x\text{RuO}_3$ for Ca rich compositions. Inset: zoomed low field range.

equation of state. The Arrott plots for these two materials are shown in Fig. 18. It is clear that for the sample with $x = 0.6$ there is a different from zero magnetisation at $H = 0$ at low temperatures. The plot allows to determine from a suitable isotherm the Curie temperature $T_C \simeq 23(1)$ K. The Curie temperatures for the samples with different calcium concentrations determined from the adequate Arrott plots are shown on the $B = 0$ phase diagram in Fig. 3 in the main text. Moreover, there is no any isotherm which leads to the different from zero magnetisation at $H = 0$ for the $\text{Sr}_{1-x}\text{Ca}_x\text{RuO}_3$ compounds with $x \geq 0.8$, including pure CaRuO_3 (not shown) which means that all these compounds are essentially in the paramagnetic state. The Arrott plot for the $x = 0.8$ material is shown in Fig. 18(bottom). The essentially paramagnetic ground state of CaRuO_3 , at least down to 1.8 K, was also inferred from the results of ^{99}Ru Mössbauer effect investigations.²⁴ This of course does not excludes

existence of some very small amount of magnetic clusters, detection of which is below the sensitivity of both methods.

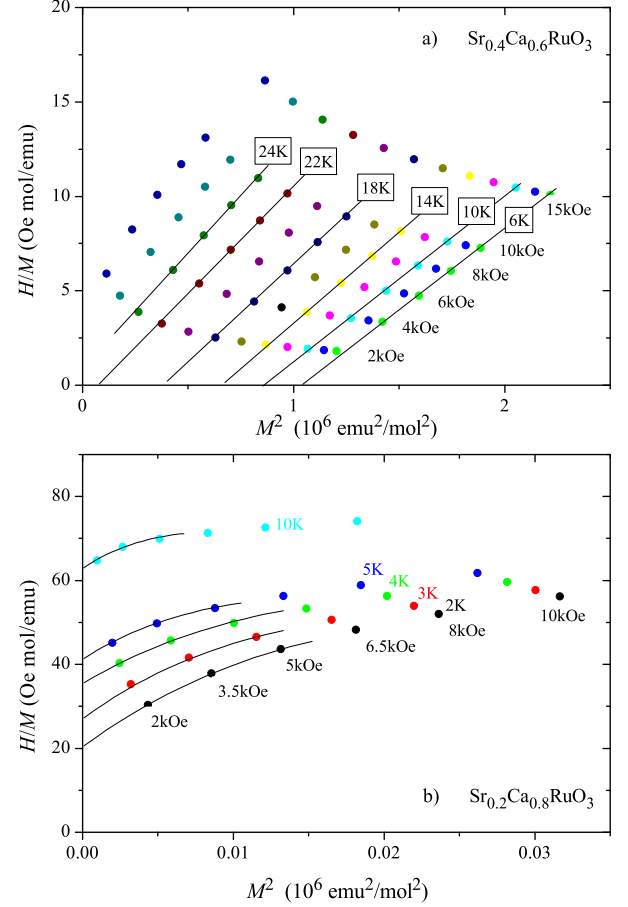


FIG. 18: Arrott plot for $\text{Sr}_{0.4}\text{Ca}_{0.6}\text{RuO}_3$, showing that the sample is ferromagnetic with T_C around 23 K (top) and the similar plot for $\text{Sr}_{0.2}\text{Ca}_{0.8}\text{RuO}_3$ (bottom) without bulk ferromagnetism present down to 2 K.

As it was already mentioned, to have the proper notion about the magnetic properties of the $\text{Sr}_{1-x}\text{Ca}_x\text{RuO}_3$ compounds, one has to take into account the results of μSR investigations.^{26,27} They show that whereas the compounds with calcium concentration $x \leq 0.6$ are homogeneous ferromagnets, which means that all Ru atoms carry magnetic moments which takes part in the ferromagnetic ordering. Materials with $x \geq 0.65$ are magnetically not homogeneous, it means they contain both magnetic and nonmagnetic fractions. In addition, the already mentioned results of magnetization measurements of thin film²⁵ show that the ferromagnetic phase is extended by the random disorder which could be understood by formation of the inhomogeneous ferromagnetic material built up of ferromagnetic clusters diluted in the paramagnetic matrix. Presumably, since the Sr and Ca atoms are randomly distributed in the perovskite lattice, the magnetic fraction built up of the ferromagnetic clusters is caused

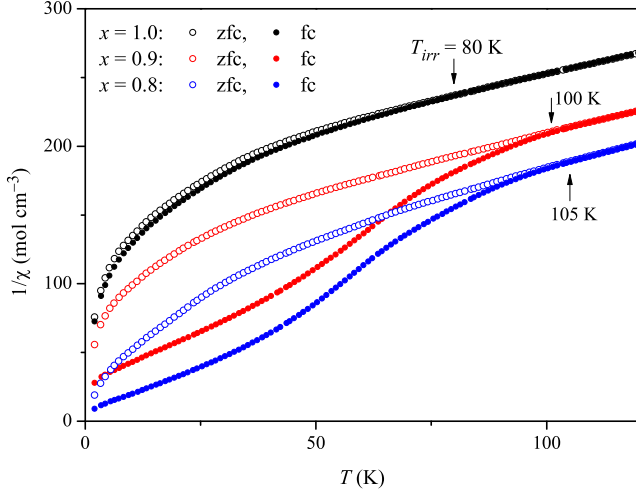


FIG. 19: Zero-field cooled (open circles) and field cooled (solid dots) susceptibility measured at 50 Oe and shown as $1/\chi$, for Ca-rich members of $\text{Sr}_{1-x}\text{Ca}_x\text{RuO}_3$.

by the regions which contain in average more Sr atoms in the nearest surrounding of Ru then anticipated from the nominal concentration. These regions are more favorable for the ferromagnetic order. Formation of such clusters in some regions of the sample which are more susceptible to the ferromagnetic order could be the reason of the difference between a field cooled (FC) and a zero field cooled (ZFC) susceptibilities in the weak magnetic fields of 50 Oe, observed in all investigated samples including pure CaRuO_3 (Fig. 19). Moreover, the existence of the ferromagnetic clusters in the paramagnetic CaRuO_3 was suggested by the results of the neutron scattering experiments.²⁸ In the opinion of the authors of this reference such clusters can be induced by the defects in the crystalline structure.

Taking all of that into account one can conclude that even the essentially paramagnetic materials which we expect in the high calcium concentration side can have small ferromagnetic clusters embodied into the paramagnetic medium. Formation of these clusters probably starts in the range of temperature where the zero-field cooled and field cooled susceptibility diverges. The temperature of irreversibility is marked by arrows in Fig. 19. At high temperatures these clusters are independent and behave as large superparamagnetic particles, but at low temperatures even with very weak interaction the system can freeze forming the cluster glass phase.

B. ^{99}Ru Mössbauer spectroscopy

The magnetic properties of $\text{Sr}_{1-x}\text{Ca}_x\text{RuO}_3$ system were also investigated using the ^{99}Ru Mössbauer spectroscopy. These investigations were performed for materials which cover the whole range of calcium concentrations and their results will be the subject of a separate

publication.⁵⁵ In this report only the Mössbauer spectra for materials with the composition $x = 0.6$ and $x = 0.8$ are presented (Fig. 20). Both of them were obtained with the ^{99}Rh source in the matrix of metallic ruthenium at $T = 4.2$ K.

Spectrum obtained for the $x = 0.6$ sample was analyzed taking into account the existence of the hyperfine magnetic field (H_{hf}) at each ruthenium site with distribution of H_{hf} values caused by different surroundings of ruthenium by calcium and strontium atoms. This spectrum confirms that $\text{Sr}_{0.4}\text{Ca}_{0.6}\text{RuO}_3$ is homogeneously magnetically ordered. In the contrary, the Mössbauer spectra for the $x = 0.8$ material was analysed as a non-magnetic spectrum which, even taking into account an extremely small and unresolved quadrupole splitting in the resonance absorber and source, looks like a single narrow resonance line. This spectrum confirms nonmagnetic (paramagnetic) state of $\text{Sr}_{0.2}\text{Ca}_{0.8}\text{RuO}_3$ at 4.2 K. Nevertheless, this does not contradict a possible existence of the ferromagnetic clusters mentioned in the previous section with concentration below approximately 3%.

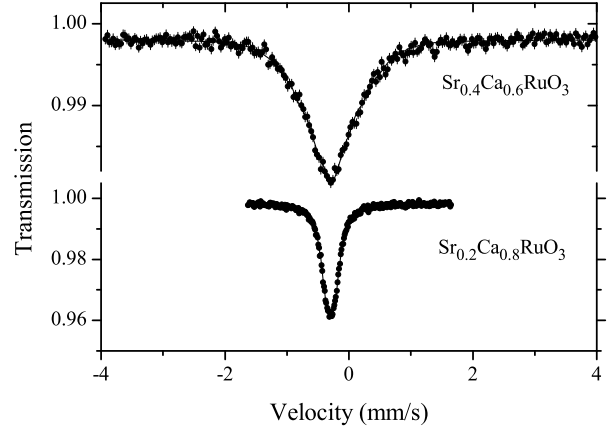


FIG. 20: ^{99}Ru Mössbauer spectra for $\text{Sr}_{0.4}\text{Ca}_{0.6}\text{RuO}_3$ and $\text{Sr}_{0.2}\text{Ca}_{0.8}\text{RuO}_3$ at 4.2 K. For the latter no hyperfine magnetic field is measurable, while for the former, significant broadening of the spectrum is caused by magnetic hyperfine field.

C. Numerical data inferred from C/T and $\rho(t)$ analysis

This section contains four Tables of collected almost all results obtained from the analysis of the specific heat and electrical resistivity.

TABLE I: Results of specific heat analysis using the SCR model of T. Moriya.

compound	B (T)	T_{LFL} (K)	y_0	y_1	T_0 (K)	γ_0 (mJ·mol ⁻¹ ·K ⁻²) ^a
CaRuO ₃	0	1.6(2)	0.1001(37)	5.25(26)	215.4(3.0)	10
	0.27 ^b	—	—	—	—	—
	0.5	0.7(1)	0.0572(19)	2.40(17)	257.0(2.7)	10
	1	1.3(2)	0.0954(36)	4.68(26)	218.6(3.0)	10
	3	2.1(2)	0.1652(14)	7.77(74)	179.3(6.2)	10
Sr _{0.2} Ca _{0.8} RuO ₃	0 ^b	—	—	—	—	—
	0.2 ^b	—	—	—	—	—
	0.5	0.9(1)	0.0727(19)	2.54(13)	227.8(2.0)	10
	1	2.0(2)	0.1761(84)	6.71(97)	164.9(2.0)	10
	3	3.9(2)	0.7067(150)	22.2(4.2)	79.6(11.0)	10

^aParameter fixed during the least-squares fitting procedure.^bData at this field could not be well reproduced using only this model, and for this reason the parameters are not given to avoid distorted values.TABLE II: Resistivity analysis using $\rho = \rho_0 + a_2 T^2$ and $\rho = \rho_0 + a_{5/3} T^{5/3}$ dependencies.

compound	B (T)	T_{LFL} ^b (K)	ρ_0 (10 ⁻⁵ Ω·cm)	a_2 (10 ⁻⁷ Ω·cm·K ⁻²)	$a_{5/3}$ (10 ⁻⁷ Ω·cm·K ^{-5/3})	T range ^c (K)
CaRuO ₃	0	1.6(2)	3.992(2)	3.467(6)	4.646(9)	1.52–8.75
	0.27	—	—	—	—	—
	0.5	—	—	—	4.608(7)	below 0.8–9.54
	1	—	—	—	4.646(7)	1.43–9.51
	3	1.9(1)	4.067(4)	3.087(15)	4.531(7)	2.22–9.93
	6	3.0(2)	4.224(4)	2.457(10)	4.281(5)	2.9–10.9
	9	3.5(2)	4.409(4)	2.220(4)	4.075(9)	4.77–11.6
Sr _{0.2} Ca _{0.8} RuO ₃	0	—	—	—	3.154(17)	below 0.8–9.86
	0.2	—	—	—	3.168(17)	below 0.8–9.70
	0.5	—	—	—	3.154(40)	below 0.8–10.5
	1	2.4(2)	18.729(8)	2.58(41)	3.194(17)	2.52–10.52
	3	4.2(2)	18.724(4)	1.804(58)	3.084(20)	3.78–10.55
	6	6.7(2)	18.715(3)	1.443(12)	2.950(20)	4.53–11.4
	9	8.5(2)	18.729(3)	1.274(6)	2.787(20)	4.47–11.7

^aGiven uncertainties of ρ_0 , a_2 , $a_{5/3}$ are statistical errors of fitting using the least-square method. The systematic errors related with the geometry of samples reach 10%.^bThe maximal T where T^2 law well reproduces experimental data.^cThe range of T where the $T^{5/3}$ law well reproduces experimental data.

TABLE III: Results of resistivity analysis using the SCR model $\rho = \rho_0 + \rho_{SCR}$ and temperature range from 0.6 to 5 K.

compound	B (T)	ρ_0 ($10^{-5} \Omega \cdot \text{cm}$)	a_{SCR} ($10^{-5} \Omega \cdot \text{cm}$)
CaRuO ₃	0	4.007(2)	812.6(8.0)
	0.5	4.005(2)	812.6(5.1)
	1	4.012(2)	824.8(4.0)
	3	4.080(2)	804.0(8.1)
	6	—	—
	9	—	—
Sr _{0.2} Ca _{0.8} RuO ₃	0	—	—
	0.5	18.743(3)	505.8(5.8)
	1	18.747(4)	497.3(8.3)
	3	18.729(4)	476.9(8.3)
	6	—	—
	9	—	—

TABLE IV: Results of resistivity analysis using the Anderson model $\rho = \rho_0 + a_A T^2 / (T + T_0)$ and temperature range from 0.6 to 24 K.

compound	B (T)	ρ_0 ($10^{-5} \Omega \cdot \text{cm}$)	a_A ($10^{-5} \Omega \cdot \text{cm}$)	T_0 (K)
CaRuO ₃	0	4.002(2)	0.5355(9)	15.7(1)
	0.5	4.000(2)	0.5350(10)	15.7(1)
	1	4.013(2)	0.5436(9)	16.3(1)
	3	4.069(2)	0.5430(11)	16.8(1)
	6	4.215(2)	0.5618(11)	19.1(1)
	9	4.397(2)	0.5932(14)	22.8(1)
Sr _{0.2} Ca _{0.8} RuO ₃	0	18.747(3)	0.3491(22)	14.2(3)
	0.5	18.730(3)	0.3499(18)	14.2(2)
	1	18.726(3)	0.3523(24)	14.4(3)
	3	18.713(3)	0.3676(28)	16.2(3)
	6	18.693(3)	0.3955(35)	20.0(4)
	9	18.706(3)	0.4298(50)	25.2(5)